OXFORD

SOT | Society of Toxicology
www.toxsci.oxfordjournals.org

TOXICOLOGICAL SCIENCES, 155(1), 2017, 43–60

doi: 10.1093/toxsci/kfw178
Advance Access Publication Date: September 14, 2016
Research article

High-Content Analysis Provides Mechanistic Insights into the Testicular Toxicity of Bisphenol A and Selected Analogues in Mouse Spermatogonial Cells

Shenxuan Liang,* Lei Yin,*,† Kevin Shengyang Yu,*,2 Marie-Claude Hofmann,‡ and Xiaozhong Yu*,1

*Department of Environmental Health Science, College of Public Health, University of Georgia, Athens, Georgia; †ReproTox Biotech LLC, 111 Riverbend Drive, Athens, Georgia; and ‡Department of Endocrine Neoplasia & Hormonal Disorders MD Anderson Cancer Center, 1515 Holcombe Blvd, Unit no. 1105 Houston, Texas

[1]To whom should be addressed to Department of Environmental Health Science, College of Public Health, University of Georgia, 150 Green Street, Athens, GA 30602, USA. Fax: 706.542.7472. E-mail: yuxz@uga.edu.

[2]Current Address: UCSF Medical School, 513 Parnassus Ave, San Francisco, CA 94143-0410.

ABSTRACT

Bisphenol A (BPA), an endocrine-disrupting compound, was found to be a testicular toxicant in animal models. Bisphenol S (BPS), bisphenol AF (BPAF), and tetrabromobisphenol A (TBBPA) were recently introduced to the market as alternatives to BPA. However, toxicological data of these compounds in the male reproductive system are still limited so far. This study developed and validated an automated multi-parametric high-content analysis (HCA) using the C18-4 spermatogonial cell line as a model. We applied these validated HCA, including nuclear morphology, DNA content, cell cycle progression, DNA synthesis, cytoskeleton integrity, and DNA damage responses, to characterize and compare the testicular toxicities of BPA and 3 selected commercial available BPA analogues, BPS, BPAF, and TBBPA. HCA revealed BPAF and TBBPA exhibited higher spermatogonial toxicities as compared with BPA and BPS, including dose- and time-dependent alterations in nuclear morphology, cell cycle, DNA damage responses, and perturbation of the cytoskeleton. Our results demonstrated that this specific culture model together with HCA can be utilized for quantitative screening and discriminating of chemical-specific testicular toxicity in spermatogonial cells. It also provides a fast and cost-effective approach for the identification of environmental chemicals that could have detrimental effects on reproduction.

Key words: bisphenol A; bisphenol S; bisphenol AF; and tetrabromobisphenol A; C18-4 spermatogonial cell line; high-content analysis; cell cycle; DNA damage responses; cytoskeleton.

Bisphenol A (BPA) is a high production volume chemical, and worldwide used in food and beverage packaging materials, dental sealants and composite fillings, medical devices and thermal paper (Rochester, 2013). Human exposure to BPA occurs through ingestion, inhalation, and dermal contact from a variety of sources (Kang *et al.*, 2006; Vandenberg *et al.*, 2007). BPA and its metabolites are widely distributed in humans and animals (Calafat *et al.*, 2005; Melzer *et al.*, 2010), and were detected in more than 90% of urine samples from the U.S. population in the 2003–2004 and 2005–2006 National Health and Nutrition Examination Survey (Calafat *et al.*, 2008; Lakind and Naiman, 2011). As a known endocrine disruptor, BPA has been shown to interfere with hormonal and homeostatic systems, and BPA levels in human urine have been correlated with various diseases and adverse health outcomes (Braun *et al.*, 2011; Carwile and Michels, 2011; Ehrlich *et al.*, 2012; Lang *et al.*, 2008; Lassen *et al.*, 2014). BPA exposure has also been associated with reproductive dysfunctions, including reduction of testicular weight and sperm count,

alterations of hormone levels, and impairment of spermatogenesis (Jin *et al.*, 2013; Pacchierotti *et al.*, 2008; Sakaue *et al.*, 2001; Tiwari and Vanage, 2013; Wang *et al.*, 2016). The mechanism of action of BPA has been investigated with respect to its estrogenic activity, such as effects on steroid hormone synthesis, and androgen receptor (AR) antagonism (Kitamura *et al.*, 2005; Lee *et al.*, 2003; Vinggaard *et al.*, 2008; Zhang *et al.*, 2011). Due to public concern about these potential adverse effects of BPA, the U.S. Food and Drug Administration (FDA) has enforced restrictions on the manufacture and usage of BPA (FDA, 2012, 2013). As a result, the production of BPA analogues has greatly increased and is expected to rise in the future. With inadequate data on their toxicities, BPA analogues have gradually been used for the manufacture of a wide variety of consumer products. However, because of their structural similarities with BPA, the safety of these analogues is a subject of debate, and there is accumulating evidence that they also have the potential to be endocrine disruptors (Usman and Ahmad, 2016). To date, the health risks of BPA analogues need to be fully evaluated.

There are significant challenges to understanding the health risks associated with thousands of diverse compounds entering the environment. Studying reproductive toxicity *in vivo* is usually complicated, expensive, and time-consuming; they also involve extensive animal use, which significantly limits the number of chemicals to be tested. There is thus an urgent need to develop effective and practical tools for early screening of chemicals with potential adverse effects using high-throughput, low-cost methodologies that ensure high predictability of human biological responses (Parks Saldutti *et al.*, 2013). Recently, *in vitro* testicular models have been introduced to environmental chemical safety assessment to improve the predictability of chemical-induced testicular toxicity in human and elucidate mechanisms of chemical toxicity (Harris *et al.*, 2015; Hofmann *et al.*, 2005a; Parks Saldutti, et al., 2013; Wegner *et al.*, 2013, 2014; Yu *et al.*, 2003, 2005, 2009). Some of these *in vitro* models form a testicular-like multilayered architecture that mimics *in vivo* characteristics of seminiferous tubules (Yu *et al.*, 2003, 2005). However, these *in vitro* primary testicular cell co-culture models still have the disadvantage of employing animals for the isolation of testicular cells. In addition, complicated isolation procedures lead to inconsistency of primary testicular cells (Wegner *et al.*, 2013). In this study, we used a spermatogonial cell line (C18-4) to examine and compare the toxicity profiles of BPA and some of its analogues. The C18–4 germline cell line was previously established from type A spermatogonia isolated from 6-day-old mouse testes (Hofmann *et al.*, 2005a,b; Kokkinaki *et al.*, 2009).

There is a need for improved *in vitro* methods to meet the challenges associated with the increasing push to predict the toxicity of chemicals. The Environmental Protection Agency has initiated a ToxCast project integrating *in vitro* high-content and high-throughput toxicity assessment to characterize the toxicological profiles of thousands of chemicals (Auerbach *et al.*, 2016; Karmaus *et al.*, 2016; Kavlock *et al.*, 2012; Paul Friedman *et al.*, 2016). High-content analysis (HCA) has been demonstrated to be particularly useful for toxicity testing and prediction as it enables measurements of multiple, early toxicological mechanisms by characterizing co-expression of multiple molecules, as well as quantification and visualization of the spatial and temporal dynamic processes of cellular events. HCA has been successfully applied to the prediction of drug-induced human hepatotoxicity, and this highly specific and sensitive assay has shown high concordance with human data (O'Brien *et al.*, 2006; Schoonen *et al.*, 2005; Xu *et al.*, 2004, 2008). Furthermore, the HCA enables comparisons of the effectiveness of various assay parameters, detects high-risk chemicals and the sequences of cellular events. By linking chemical-biological interactions with sequential key events at multiple biological responses, adverse outcome pathways provide a mechanism-based framework to support the hazard assessment of chemicals (Ankley *et al.*, 2010; Perkins *et al.*, 2015).

The purpose of this study was to develop an automated multi-parametric screening method and to optimize protocols for cell treatment, high-content imaging, and image analysis of the C18-4 spermatogonial cells. We applied this validated HCA approach to characterize and compare the testicular toxicities of BPA and 3 selected commercially available BPA analogues: bisphenol S (BPS), bisphenol AF (BPAF), and tetrabromobisphenol A (TBBPA). We concurrently compared a wide spectrum of cellular and molecular events that potentially lead to impaired male reproductive function, including nuclear morphology, DNA content, cytoskeletal integrity, cell cycle, and DNA damage responses in a dose and time-dependent manner. Overall, our results demonstrated that this *in vitro* model combined with HCA can be utilized for a quantitative screening of chemical effects in spermatogonial cells and enable rapid and cost-effective measurement of the multidimensional biological profile of toxicity.

MATERIALS AND METHODS

Chemicals

Dulbecco's Modified Eagle Medium (DMEM), and Penicillin-Streptomycin were purchased from GE Healthcare Life Sciences (Logan, Utah). Fetal bovine serum (FBS), 2,2-bis(4-hydroxy-3-methylphenyl) propane (BPA, $\geq$ 99%), 4,4′-sulfonyldiphenol (BPS, 98%), 3,3′,5,5′-TBBPA (97%), and neutral red (NR) were purchased from Sigma-Aldrich (St Louis, Missouri). 4,4′-(hexafluoroisopropylidene) diphenyl (BPAF, 98%) was purchased from Alfa Aesar (Ward Hill, Massachusetts). The chemical structures of these compounds are shown in Figure 1 (Chen *et al.*, 2016; Colnot *et al.*, 2014). 5-Bromo-2′-deoxyuridine (BrdU, 99%) was purchased from Thermo Scientific (Waltham, Massachusetts). Paraformaldehyde (4% in phosphate-buffered saline) was purchased from Boston Bioproducts (Ashland, Massachusetts).

Cell culture and treatment

The mouse C18-4 spermatogonial cell line was established from germ cells isolated from the testes of 6-day-old Balb/c mice. This cell line shows morphological features of type A spermatogonia, expresses germ cell-specific genes such as GFRA1, Dazl and Ret, which are markers specific for germ cells in the testis (Hofmann *et al.*, 2005a,b). Cells were maintained in DMEM medium composed of 5% FBS, and 100 U/ml streptomycin and penicillin in a 33°C, 5% CO_2 humidified environment in a sub-confluent condition with passaging every 3–4 days. When they reached 70–80% confluence, cells were inoculated with 1.2×10^4 per well in a 96-well plate. Cells were cultured overnight and treated with various concentrations of BPA, BPS, BPAF and TBBPA for the indicated doses and time periods.

Cell viability

Cell viability was determined by measuring the capacity of cells to take up NR. NR can be retained inside the lysosomes of viable cells, while the dye cannot be retained if the cells dies. Dye retention is proportional to the number of viable cells, and can be

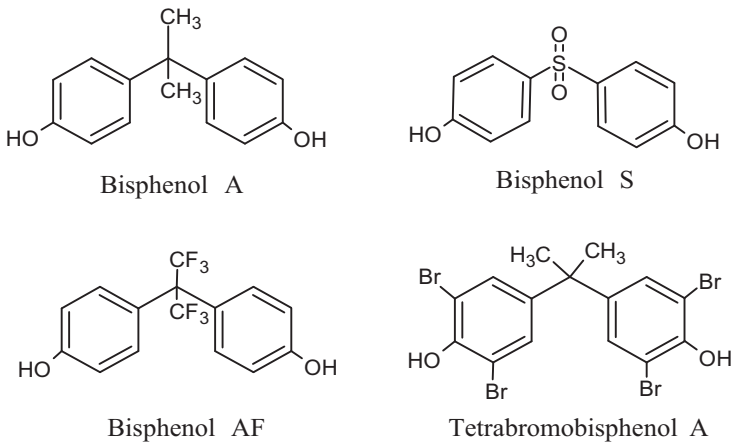

FIG. 1. Chemical structures of BPA, BPS, BPAF, and TBBPA (Chen *et al.*, 2016; Colnot *et al.*, 2014).

measured based on NR absorbance (Repetto *et al.*, 2008; Yu *et al.*, 2009). Significant changes in cell viability were determined using a 1-way analysis of variance (1-way ANOVA) followed by Tukey-Kramer multiple comparison tests. Briefly, cells were treated with various concentrations of BPA, or BPS, (50, 100, 200 and 400 μM), and BPAF or TBBPA (25, 50, 75 and 100 μM) for different length of time (24–72 h). Cells treated with vehicle (0.05% DMSO) were used as the reference group with cell viability set as 100%. After treatments, the culture medium was removed and fresh medium containing NR (50 μg/ml) was added. Following 3 h incubation, cells were washed with phosphate buffered saline (PBS) and NR was eluted with 100 μl of a 0.5% acetic acid/50% ethanol solution. The plate was gently rocking on a plate shaker, and absorbance values were measured at 540 nm with a Synergy HT microplate reader (BioTek, Vermont). Cell viability was expressed as percentage of the mean of vehicle controls after subtracting the background control.

Fluorescence staining and image acquisition

For cell cycle analysis, cells were incubated with BrdU (40 μM) for 3 h prior to fixation. Cells in the controls reached 100% confluence at the time of harvest. Cells were then fixed with 4% paraformaldehyde for 30 min at room temperature, followed by 3 times washing with PBS. Cells were then acidified with a 4N HCl/Triton X-100 solution for 30 min at room temperature. After neutralization with $Na_2B_4O_7$ solution for 10 min, cells were washed twice with PBS, and blocked with 3% BSA in PBS. Cells were then incubated with a mouse anti-BrdU antibody (Thermo Scientific, Massachusetts) in PBS/BSA/0.5% Tween 20 overnight at 4 °C. After washing twice with PBS/BSA, cells were incubated with a goat anti-mouse DyLight 488 and the DNA staining dye Hoechst 33342 (Thermo Scientific, Massachusetts) in PBS/BSA solution for 90 min at room temperature.

For DNA damage responses and cytoskeleton analysis, cells treatments and fixation were the same as described above. After fixation, cells were permeabilized by 0.1% Triton X-100 in PBS, then incubated with mouse anti-phospho-Histone-H2AX (Ser139) (γ-H2AX) (Millipore, Massachusetts) in PBS/BSA/0.5% Tween 20 solution overnight at 4 °C. After washing twice with PBS/BSA, cells were incubated with goat anti-mouse Dylight 650 (Thermo Scientific, Massachusetts), and Hoechst 33342 in PBS/BSA solution for 90 min at room temperature. Prior to image acquisition, cells were stained with Alexa Fluor 488 Phalloidin (Cell Signaling, Massachusetts) for F-actin staining for 30 min at room temperature.

Multichannel images were automatically acquired using an Arrayscan VTI HCS reader with HCS Studio 2.0 Target Activation BioApplication module (Thermo Scientific, Massachusetts). Forty-nine fields per well were acquired at 20× magnification using Hamamatsu ROCA-ER digital camera in combination with 0.63× coupler and Carl Zeiss microscope optics in auto-focus mode. Channel 1 (Ch1) applied the BGRFR 386_23 for Hoechst 33342 that was used for auto-focus, object identification and segmentation. Image smoothing was applied to reduce object fragmentation prior to object detection in Ch1. Border objects were excluded. For BrdU staining, channel 2 (Ch2) applied the BGRFR 549_15 for BrdU. For F-actin and γ-H2AX staining, Ch2 applied the BGRFR 485_20 for F-actin and channel 3 (Ch3) applied the BGRFR 650_13 for γ-H2AX.

High-content images analysis

Multi-Channel images were analyzed using HCS Studio 2.0 TargetActivation BioApplication. Change in nuclear morphology is an early event of the cellular response, and is associated with cellular function (Elmore, 2007; Webster *et al.*, 2009; Zhivotosky and Orrenius, 2001). Single-cell based HCA provided multiple parameters to characterize the nucleus, including the number, nuclear area, shape, and total or average intensity. Nuclear shape measurement included P2A and length–width ratio (LWR) parameters. P2A is a shape measurement based on the ratio of the nuclear perimeter squared to 4π*nucleus area (perimeter^2/4 π * nucleus area), which evaluates nucleus smoothness. LWR measures the ratio of the length to the width of the nucleus, which evaluates nucleus roundness. For a fairly round and smooth object, the values for P2A and LWR are around 1.0. Total intensity was defined as total pixel intensities within a cell in the respective channel; the average intensity was defined as the total pixel intensities divided by the area of a cell in the respective channel. With 49 fields of each well, at least 5000 cells were analyzed per well and single-cell based data for each channel were exported for further statistical analysis. The experiments were performed with at least 3 biological replicates and repeated twice.

HCA-based cell cycle analysis was conducted as recently reported by Roukos et al (Roukos *et al.*, 2015). The frequency distributions of total DNA intensity of all individual nuclei were calculated and plotted for each experimental condition in a

custom script written in Python 3.5.2 (Python Software Foundation, Oregon; this script is freely available from the authors upon request). Cell cycle profiles with discrete sub-G1 (apoptotic cells), G0/1, S or G2/M populations in the controls and treatments were determined by the selections of appropriate thresholds of these gates as reported (Roukos *et al.*, 2015).

Statistical analysis

All data obtained from the HCS Studio 2.0 TargetActivation BioApplication were exported and further analysis was conducted using the JMP statistical analysis package (SAS Institute, North Carolin). Objects with nuclear area $<50\,\mu M^2$ or $>800\,\mu M^2$ were excluded in order to remove cell debris and clumps. For each plate, the vehicle control showed consistent measurement for all endpoints tested. For intra-plate normalization, each sample value was normalized to the overall scaling factors, which was the mean of median values of vehicle control (0.05% DMSO) in each plate. The parameters from single-cell based imaging were quantified, and averaged for each well condition. For the mega or multi-nuclei identification in the automatic HCA, nuclei with enlarged nuclear area ($\geq 500\,\mu m^2$) and irregular nuclear shape (P2A $\geq$ 1.35) were identified, and the percentages were calculated. BrdU positive cells were set by the total intensity of BrdU in the control over 20,000 pixels. γ-H2AX positive cells were set by the total intensity of γ-H2AX in the control over 120,000 pixels. Data were presented as mean ± SD. Statistical significance was determined using 1-way ANOVA followed by Tukey-Kramer all pairs comparison. A P value $< .05$ denoted a significant difference compared with the vehicle control (*).

To examine the relationship between the cytoskeleton and DNA damage responses, Spearman correlation analysis was conducted between log-transformed total intensity of F-actin and log-transformed total intensity of γ-H2AX at 24, 48 and 72 h.

The 20% maximal effect concentration (EC20) and median lethal concentration (LC50) were calculated with a curve-fitting program using GraphPad Prism 5 (San Diego, California). A dose-response curve fit was established based on the concentrations of chemicals that had a significant effect. The 4-parameter nonlinear regression curve fit was applied. Treatment concentrations were $\log_{10}$ transformed. For cell viability (NR assay) and cell number data (HCA), the lowest value was set to be 0% and the highest value was set to be 100%. For other markers, the lowest value was set to be controls and the highest value was set to be a maximal effect at each time point.

RESULTS

BPA and Its Analogues Induced Differential Dose- and Time-Dependent Cytotoxicity in Spermatogonial Cells

In order to select sub-lethal doses of BPA and its analogues for HCA analysis in spermatogonial cells, cell viability was measured using NR uptake assay. Figure 2 shows significant dose- and time-dependent decreases of cell viability in spermatogonial cells treated with BPA and its analogues for 24 and 48 h. BPAF reduced cell viability starting at a concentration of 25 μM, TBBPA reduced cell viability starting at a dose of 50 μM for 24 h and 25 μM for 48 h, while BPA and BPS reduced cell viability at a concentration of 100 μM for both 24 and 48 h exposure. This indicated that BPAF and TBBPA induced greater cytotoxicities, as compared with BPA and BPS. The LC50 values for 48 h were 42.2, 49.9, 132.7 and 325.3 μM for BPAF, TBBPA, BPA, and BPS, respectively. The highest concentrations of 50 μM were selected for BPA and BPS, and 25 μM were selected for BPAF and TBBPA in the following HCA experiments.

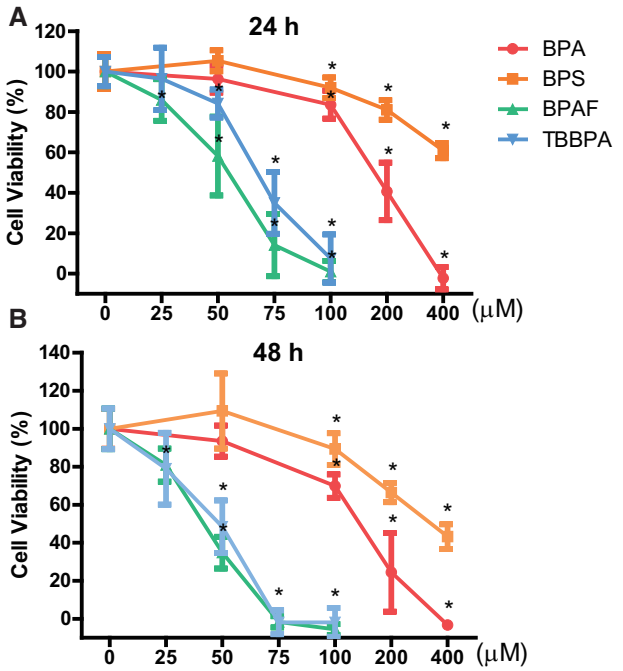

FIG. 2. Cell viability was determined by NR uptake assay in C18-4 spermatogonial cells treated with BPA, BPS, BPAF, and TBBPA. Cells were treated with various concentrations of BPA and BPS (50, 100, 200, and 400 μM), and BPAF and TBBPA (25, 50, 75 and 100 μM) for 24 **(A)** and 48 h **(B)**. Cells treated with vehicle (0.05% DMSO) were used as negative controls (0). Data were presented as mean ± SD, $n = 10$. Five replicates in 2 separate experiments were included. Statistical analysis was conducted by 1-way ANOVA followed by Tukey-Kramer multiple comparison (*$P < .05$).

BPA and Its Analogues Altered Nuclear Morphology and Cell Number

Nuclear morphology has shown to be a sensitive endpoint compared with conventional cytotoxicity assays (Martin *et al.*, 2014). In this study, we measured multiple parameters associated with nuclear morphology. Figure 3A shows representative nuclear morphologies following 72 h treatments. Notable reductions of cell numbers and increases of mega or multinucleated cell numbers were observed in the BPAF treatments at doses of 10 and 25 μM (arrows). Further quantification of the multinucleated cells using HCA demonstrated that BPAF treatment induced significant increases of multinucleated cells at doses of 25 μM for 24, 48 and 72 h (Supplementary Fig. S1). No obvious morphological change was observed for the other tested compounds. As shown in Figure 3B–D, nuclear morphological parameters obtained from HCA, including nuclear area and nuclear shape, were compared in spermatogonial cells treated with various chemicals for 24, 48 and 72 h. Significant increases of nuclear area were observed in cells treated with 25 μM BPAF for 24, 48 and 72 h, and cells treated with 50 μM BPS and 25 μM TBBPA for 72 h. BPA significantly decreased LWR at a dose of 50 μM for 72 h. BPS significantly decreased LWR and P2A at a dose of 50 μM for 72 h. However, BPAF significantly increased LWR and P2A at concentrations of 25 μM for 24 h, 10 μM for 48 h. For 72 h, BPAF significantly increased LWR at 1 μM and P2A at 10 μM. TBBPA also induced significant increases of LWR at

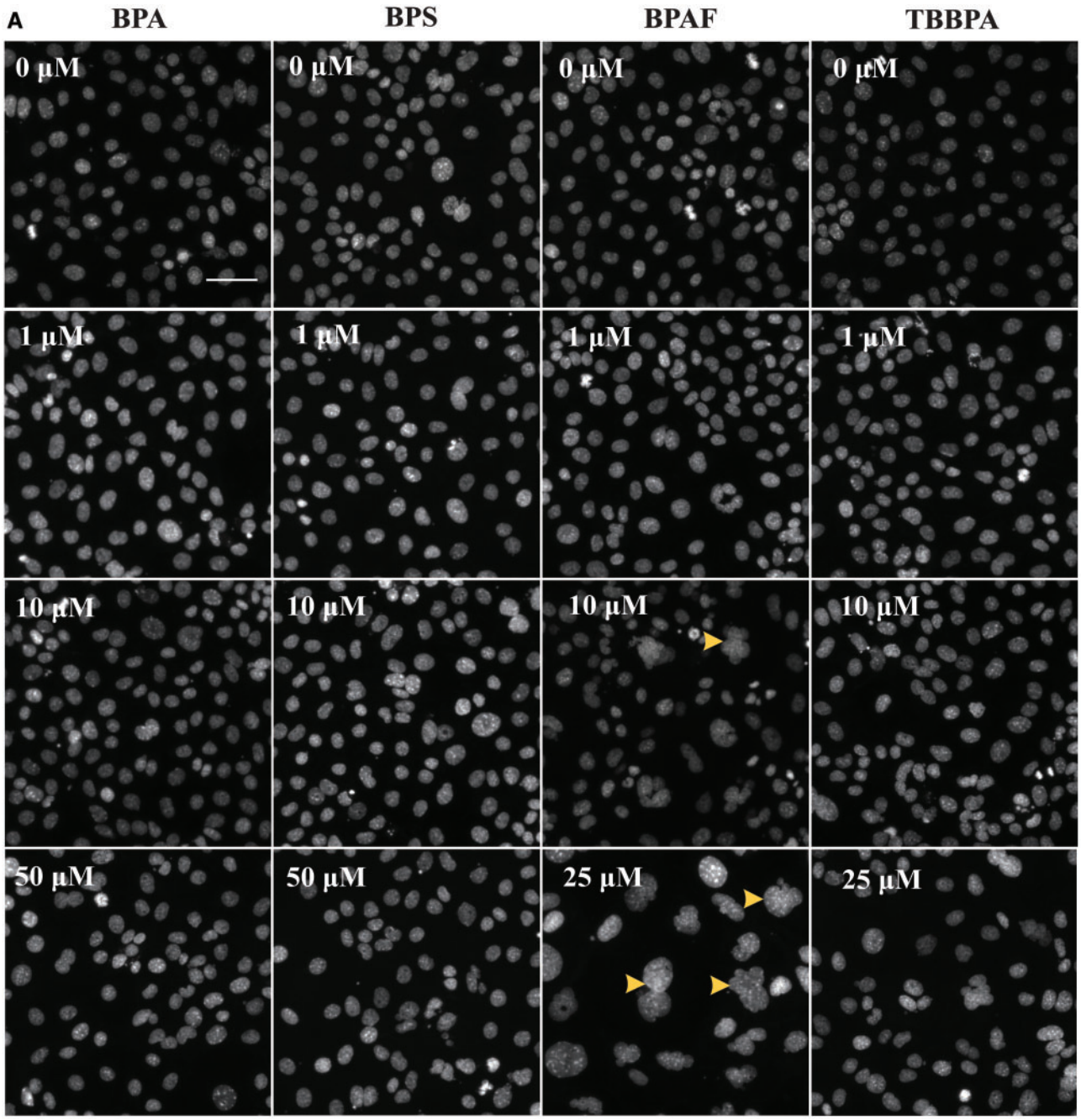

FIG. 3. HCA of nuclear morphology of C18-4 spermatogonial cells treated with BPA, BPS, BPAF and TBBPA. Cells were treated with various concentrations of BPA and BPS (0.1, 1, 10, and 50 μM), and BPAF and TBBPA (0.1, 1, 5, 10, and 25 μM). Cells treated with vehicle (0.05% DMSO) were used as negative controls (0). The nuclei of spermatogonial cells were stained with Hoechst 33342, and images were automatically obtained with a 20× objective, 49 fields per well. **A,** shows the representative images (40×) of controls and cells treated with BPA and BPS (1, 10, and 50 μM), BPAF and TBBPA (1, 10, and 25 μM) for 72 h. Arrows indicate the multinucleated cells. Scale bar = 50 μm. **B–D,** shows the quantification of absolute nuclear area (μm^2), nuclear shape, including LWR for nuclear roundness and P2A for smoothness. Data were presented as mean ± SD, $n = 9$. Three replicates in 3 separate experiments were included. Statistical analysis was conducted by 1-way ANOVA followed by Tukey-Kramer multiple comparison (*$P < .05$).

concentrations of 5, 10 and 25 μM and a significant increase of P2A at a concentration of 25 μM for 72 h.

As shown in Figure 4, BPAF and TBBPA reduced cell numbers starting at a dose of 25 μM for 24, 48 and 72 h. BPA and BPS reduced cell numbers at a dose of 50 μM for 24, 48 and 72 h. These numbers were lower than those observed with the NR assay. Notably, low doses of BPA (0.1 μM) and BPAF (0.1 and 5 μM) slightly increased cell numbers. These results suggested that for the detection of changes in cell numbers measured by HCA is more sensitive than the conventional NR uptake cytotoxicity assay.

BPA and Its Analogues Affected DNA Synthesis and Cell Cycle

The measurement of DNA content of individual cells enabled determination of the phases of the cell cycle, while the BrdU

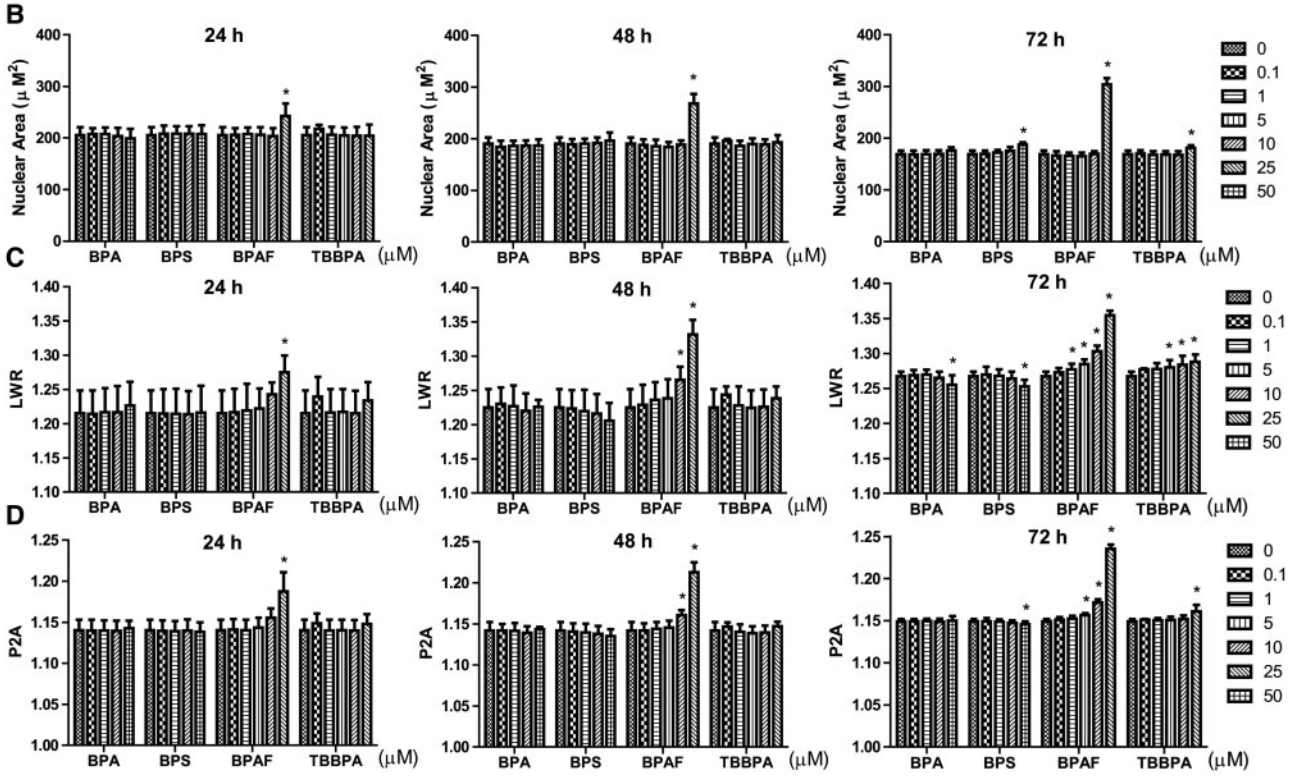

FIG. 3. Continued.

incorporation measured newly synthesized DNA. Figure 5A shows representative images of BrdU incorporation after 72 h treatments. Most multinucleated cells in the BPAF treatment were BrdU positive cells (arrows). As shown in Figure 5B, BPAF (25 μM) significantly induced total DNA intensity, by 1.3-, 1.5-, and 2.0-fold after 24, 48, and 72 h treatments as compared with the control, respectively. However, BPA, BPS, and TBBPA treatments shows no observable change of DNA total intensity. Figure 5C showed that BPS of a concentration of 50 μM and BPA of concentrations of 10, 25, 50 μM significantly decreased BrdU positive cells for 24 and 48 h, respectively, suggesting inhibitory effects of DNA synthesis from those treatments. However, BPAF treatment induced significant increases in BrdU positive cells at all 3 time-points at a concentration of 25 μM as compared with the control. No change of BrdU incorporation was observed for the TBBPA treatment.

Histogram plots of total DNA intensity were generated and the percentages of cells in each phase of the cell cycle were determined. As shown in Figure 6, the DNA intensity histogram in control groups exhibited distinguishable 2N (G0/1 phase) and 4N DNA (G2/M phase) peaks. Significant changes in the DNA histogram plot such as decreases of G0/1, and increases of S and G2/M phases in the BPAF treatment were observed. As shown in Table 1, dynamic changes of cell cycle stages in the controls across time-points, such as increases of cells in G0/1 and decreases of cells in S phase after 48 and 72 h culture were observed as compared with the control after 24 h. Cell populations in G0/1 phase were significantly decreased with a BPAF treatment of 25 μM for 24 h, 10, 25 μM for 48 and 72 h, and a TBBPA treatment of 25 μM for 24, 48, and 72 h. Significant increases of the percentage of cells in S phase were observed when cells were treated with 25 μM BPAF for 24, 48 h, and 10, 25 μM for 72 h. On the contrary, significant decreases in the percentage of cells in S phase were observed after treatments with 10 and 25 μM TBBPA for 24 and 48 h, and after treatment with 10 μM for 72 h. Accumulations of cells in G2/M phase were observed in cells treated with 10 μM BPA for 48 h, and 10 and 50 μM BPS for 48 h. A similar pattern was observed with 25 μM BPAF for 24 h, 10 and 25 μM BPAF for 48 h, and 25 μM BPAF for 72 h. Accumulations of cells in G2/M were also observed with 25 μM TBBPA for 24 and 72 h, and with doses of 5, 10 and 25 μM of TBBPA for 48 h. Significant decreases in the percentages of cells in G2/M phase were observed with a BPA treatment of 50 μM for 24 h and of 10 μM for 72 h. A BPS treatment of 10 μM for 72 h had the same effect. Finally, increases in the percentages of cells in sub-G1 phase, representing apoptotic cells, were observed with BPA at a dose of 50 μM for 72 h, with BPAF treatment at doses of 10 and 25 μM for 24 h, 25 μM for 48 h, 5and 10 μM for 72 h. TBBPA treatments of 25 μM for 48 h, and of 10, 25 μM for 72 h also increased the percentages of cells in apoptosis. Altogether, these results indicated that BPAF and TBBPA treatments at higher concentrations led to an increase of cells in the G2/M phase accompanied by an increase of apoptotic cells. Further, BPAF treatment showed unique increase of cells in S phase, which was consistent with our BrdU incorporation results. On the contrary, BPA and BPS treatments led to a decrease in the number of cells in the G2/M phase at doses of 10 or 50 μM.

BPA and Its Analogues Disrupted the Spermatogonial Cell Cytoskeleton

The cytoskeleton provides a structural framework for the cell and serves as a scaffold that determines cell shape and the organization of the cytoplasm (Sun *et al.*, 2011). We developed

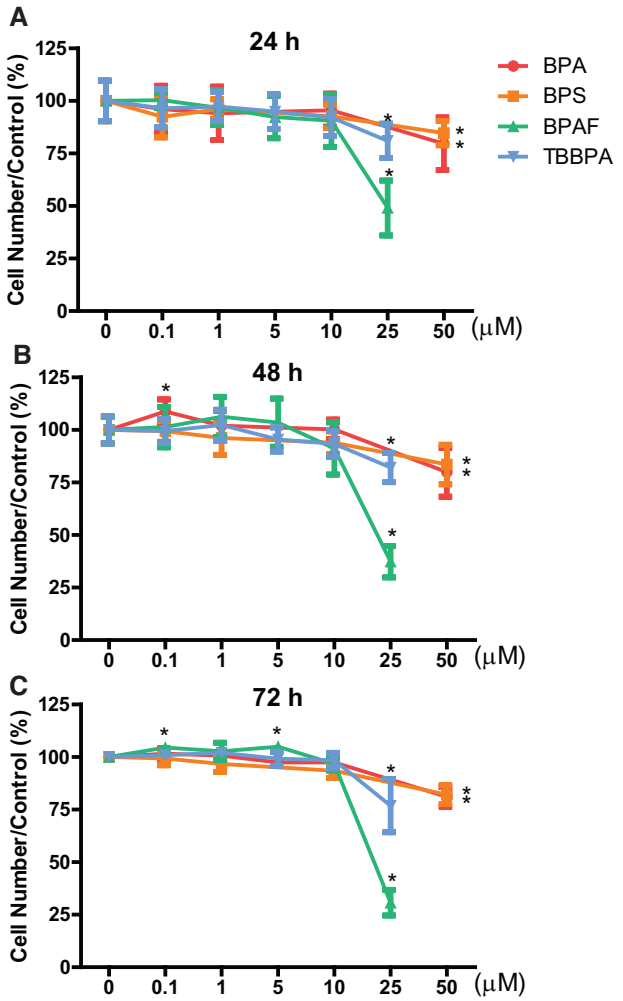

FIG. 4. HCA of cell number of spermatogonial cells treated with BPA, BPS, BPAF, and TBBPA. Cells were treated with various concentrations of BPA and BPS (0.1, 1, 10 and 50 μM), and BPAF and TBBPA (0.1, 1, 5, 10, and 25 μM) for 24 **(A)**, 48 **(B)**, and 72 h **(C)**. Cells treated with vehicle (0.05% DMSO) were used as negative controls (0). The nuclei of spermatogonial cells were stained with Hoechst 33342, and images were automatically obtained with a 20× objective, and 49 fields per well. The number of cells within 49 fields per well was counted. Data were presented as mean ± SD, $n = 9$. Three replicates in 3 separate experiments were included. Statistical analysis was conducted by 1-way ANOVA followed by Tukey-Kramer multiple comparison (*$P < .05$).

multi-parametric HCA assays to examine the effects of BPA and its analogues on the cytoskeleton of the spermatogonial cells. As shown in Figure 7A, F-actin showed a regular organization with aligned and tightly compacted structures in controls. However, BPAF and TBBPA treatments induced actin aggregate as dot-like structures with highly condensed actin staining (arrows). We further quantified the number of dot-like structures of F-actin and found significant increases in BPAF treatment at doses of 25 μM for 24, 48 and 72 h, and TBBPA treatment at doses of 25 μM for 24 and 48 h. Significant decreases of dot-like structures were observed in BPS treatment of 50 μM for 72 h (Supplementary Fig. S2). These unique structure changes were dose-dependently observed for the of BPAF and TBBPA treatments, suggesting chemical-specific effects on the cytoskeleton. Dynamic changes of total intensity of F-actin were further quantified as shown in Figure 7B. BPA and BPS (50 μM), BPAF and TBBPA (25 μM) significantly increased total intensity of F-actin at 24, 48 and 72 h exposure times. BPAF induced an approximate 2-fold increase of total F-actin intensity at 48 and 72 h exposure in comparison with other bisphenols. These data suggested that BPAF and TBBPA could potentially impair F-actin depolymerization, resulting in aberrant F-actin accumulation.

BPA and Its Analogues Induced γ-H2AX Expression, a Marker for Early DNA Damage

To further explore the potential effects of BPA and its analogues on DNA integrity, we examined γ-H2AX expression to assess early DNA damage responses in spermatogonial cells after treatments with BPA and its analogues. As shown in Figure 7A, all tested compounds induced various extent of γ-H2AX staining. BPAF induced γ-H2AX positive cells at a concentration of 25 μM. For the quantification of γ-H2AX as shown in Figure 7C, BPA treatment significantly increased the number of γ-H2AX positive cells at a concentration of 50 μM for 48 and 72 h. Both BPS (50 μM) and BPAF (25 μM) treatments significantly increased the number of γ-H2AX positive cells after 24, 48, and 72 h exposure, as compared with the control. TBBPA only induced γ-H2AX positive cells at a concentration of 25 μM for 72 h. BPAF induced a higher number of γ-H2AX positive cells, with increase of 2.5-, 3-, and 5-fold for exposures of 24, 48, and 72 h respectively as compared with the control. These data demonstrated that BPAF showed greater genotoxic potency as observed by increased expression of the DNA damage response marker γ-H2AX.

To examine the relationship between the cytoskeleton and DNA damage responses, a spearman correlation analysis was conducted based on log-transformed total intensity of F-actin and γ-H2AX. The correlation coefficients (r) are summarized in Table 2. For all 4 chemicals tested, r was positive with P values of $< .0001$, suggesting a significant and positive correlation between cytoskeleton perturbation and DNA damage responses. Thus, an increase in the intensity of F-actin staining was strongly correlated with an increase in total intensity of γ-H2AX for 24 and 48 h exposure, and moderately correlated an increase in the total intensity of γ-H2AX for 72 h, suggesting that cytoskeleton perturbation may co-occur with the DNA damage responses.

Comparison of EC20 Values of BPA and Its Selected Analogues for Different Endpoints

In order to clarify the relationship between doses of compounds, the magnitude, and type of cellular responses (endpoints), the EC20 values from different endpoints were calculated and are listed in Table 3. Similar to cell viability data obtained with the NR assay, the EC20 values of multiple endpoints obtained with the HCA were lower in all treatments, suggesting HCA-based assays identify potential targets of cytotoxic agents with improved sensitivity.

In BPA treatment, the endpoint with the lowest EC20 was cytoskeleton perturbation (7.5 μM), followed by cell number decrease (52.4 μM) and G2/M phase decrease (54.6 μM) after 24 h treatment. After 48 h treatment, the endpoint with the lowest EC20 was cytoskeleton perturbation (31.5 μM), followed by DNA damage responses (50.3 μM) and cell number decrease (50 μM). After 72 h treatment, the EC20 for multiple cellular responses was at the same dose level (50 μM). For the BPS treatment, the endpoint with the lowest EC20 was cytoskeleton perturbation (4.5 μM), followed by DNA damage responses (31.0 μM), DNA

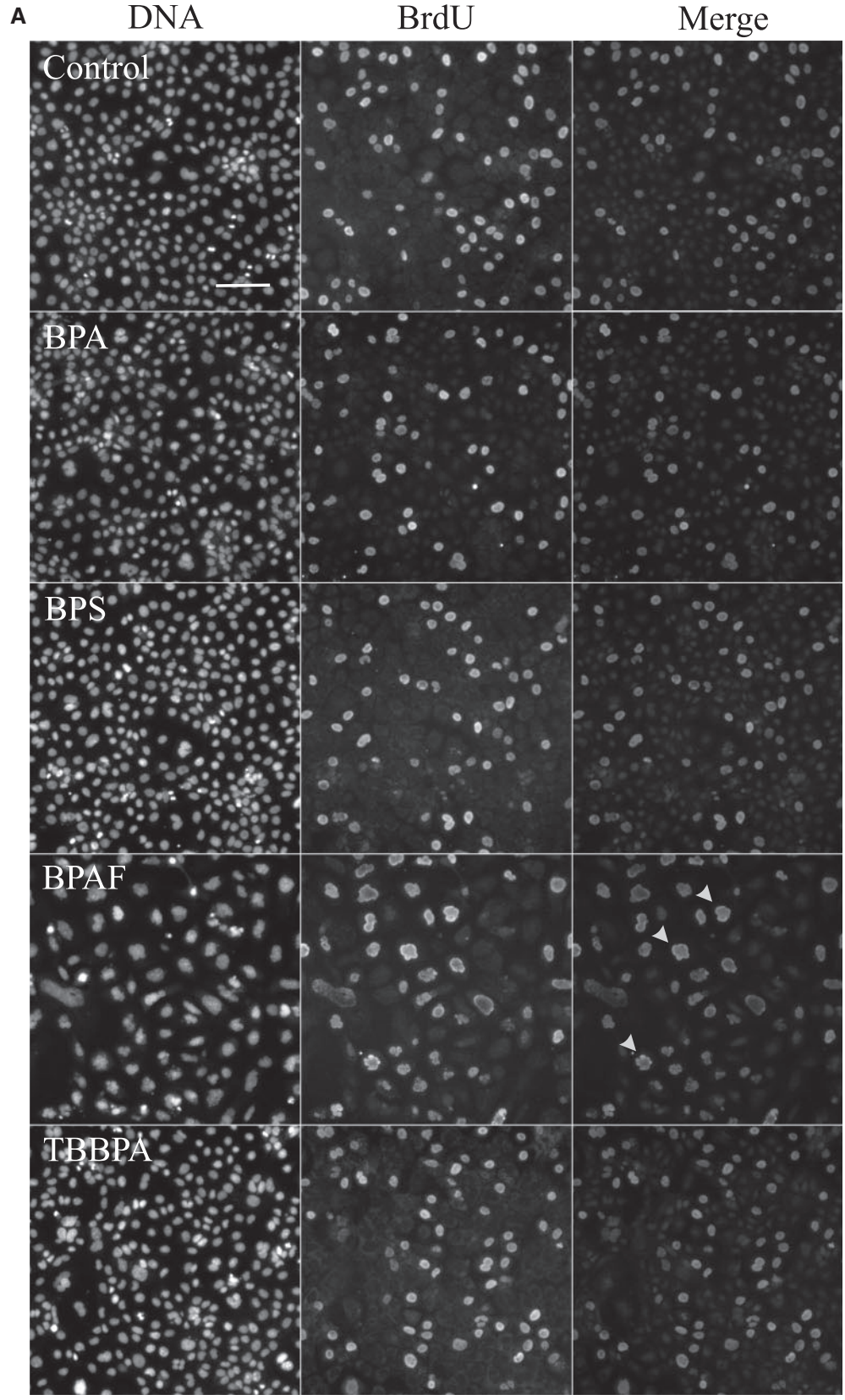

FIG. 5. HCA of DNA content and synthesis of the spermatogonial cells treated with BPA, BPS, BPAF, and TBBPA. Cells were treated with various concentrations of BPA and BPS (0.1, 1, 10, and 50 μM), and BPAF and TBBPA (0.1, 1, 5, 10, and 25 μM) for 24, 48, and 72 h. Cells treated with vehicle (0.05% DMSO) were used as negative controls (0). The nuclei were stained with Hoechst 33342. Cells were incubated with 5-bromo-2′-deoxyuridine (BrdU, 40 μM) for 3 h prior to cell fixation, and then stained with mouse anti-BrdU antibody and anti-mouse DyLight 488 for detection of BrdU incorporation (green). The nuclei were stained with Hoechst 33342 (blue). A shows the representative images of cells treated with BPA and BPS (50 μM), BPAF, and TBBPA (25 μM) for 72 h. Arrows indicate the multinucleated cells with positive BrdU staining. Scale bar = 100 μm. B shows the quantification of log-transformed total DNA intensity. C shows the quantification of BrdU-positive cells. Data were presented as mean ± SD, $n = 9$. Three replicates in 3 separate experiments were included. Statistical analysis was conducted by 1-way ANOVA followed by Tukey-Kramer multiple comparison (*$P < .05$).

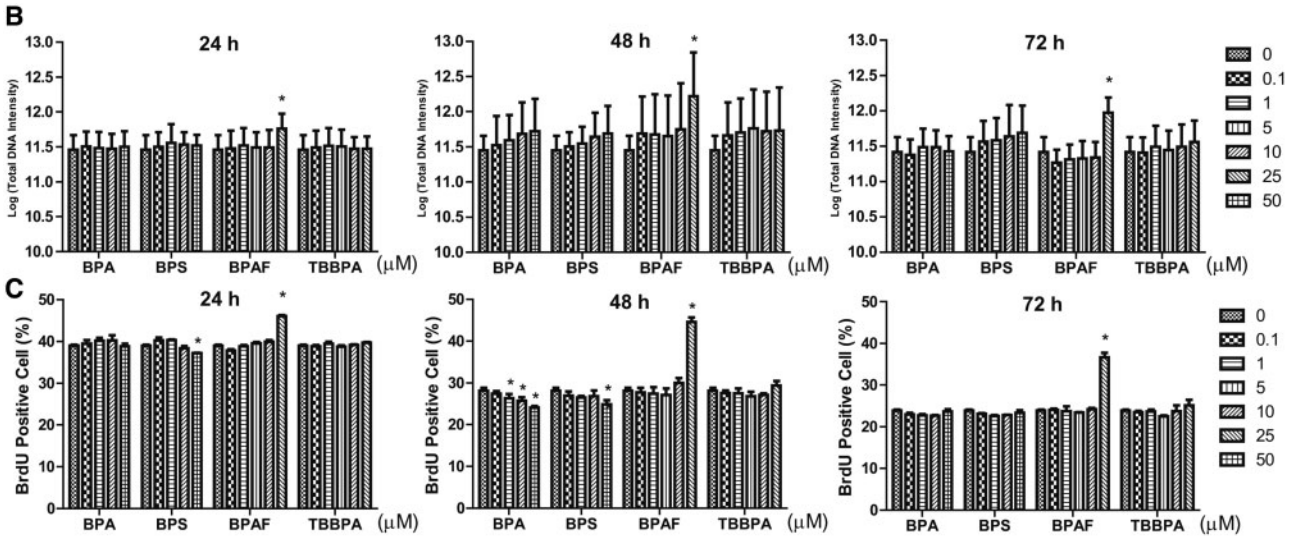

FIG. 5. Continued.

synthesis inhibition (36.9 μM) and cell number decrease (246.1 μM) after 24 h treatment. After 48 h treatment, the endpoint with the lowest EC20 was DNA damage responses (20.5 μM) followed by cytoskeleton perturbation (66.2 μM) and cell number decrease (81.4 μM). After 72 h treatment, BPS induced nuclear shape changes, cell cycle arrest, and DNA damage responses all at the same doses of 50 μM, while for cytoskeleton perturbation and nuclear area changes, the EC20 values were around 100 μM. BPAF treatment induced a wide spectrum of cellular events at a concentration of approximate 10 μM. These changes were independent of the time of exposure, and include decreases of cell numbers, changes of cell number, nuclear morphology, cell cycle perturbations, DNA synthesis facilitation, increased DNA damage responses and cytoskeleton perturbations. The induction of apoptotic cells showed the lowest EC20 values (0.4 μM) after 72 h treatment. Among these endpoints, LWR consistently showed lower EC20 values (6.1–7.6 μM), suggesting that alteration of nuclear roundness could serve as an early sensitive marker of BPAF toxicity in C-18 spermatogonial cells. For the TBBPA treatment, the endpoints with the lowest EC20 were S phase decrease (8.8 μM) followed by cytoskeleton perturbation (10.1 μM), G2/M phase increase, and cell number decrease around 25 μM after 24 h treatment. After 48 h treatment, the endpoint with the lowest EC20 was S phase decrease (5.7 μM) followed by apoptosis increase (13.7 μM), cytoskeleton perturbation (24.4 μM), cell number decrease (28.1 μM), G0/1 phase decrease (38.0 μM) and G2/M phase increase (52.2 μM). After 72 h treatment, TBBPA treatment induced various cellular responses at a concentration of ~25 μM (EC20), except for apoptosis increase. In summary, in comparison of the EC20 values of 4 bisphenols, BPAF stood out markedly, with high cytotoxicity (EC20 values ranging from 0.4 to 20 μM). TBBPA was identified as having an intermediate toxicity (EC20 values ranging from 0.3 to 47 μM). BPA and BPS were less cytotoxic (EC20 values from 4.5 to 250 μM) and the differences between these 2 compounds were minor.

DISCUSSION

Despite increasing use of BPA analogues as BPA alternatives, there are still limited data available on their reproductive toxicities. Assessing reproductive toxins poses great challenges, therefore it is urgent to develop an improved *in vitro* model to identify and assess critical biological events leading to adverse reproductive outcomes.

Cytotoxicity is a very complex process affecting multiple signaling pathways within cells. New approaches for toxicity characterization have focused on *in vitro* high-throughput and high-content assays, which enable measurement of early, sub-lethal indicators of cellular toxicity, as well as determination of the sequences and patterns of cellular events. HCA has been an effective and sensitive tool for obtaining large quantities of robust data on the multiple effects of compounds as compared with conventional cytotoxicity assays like the NR assay. Several studies demonstrated that data obtained with HCA are concordant with drug-induced toxicity in humans (O'Brien *et al.*, 2006; Schoonen *et al.*, 2005; Xu *et al.*, 2008). HCA has been widely used to assess chemical-induced mechanistic effects, and has been applied to drug discovery using specific cell type or 3D cell culture models (Anguissola *et al.*, 2014; Kameoka *et al.*, 2014; Radio *et al.*, 2008; Ramery and O'Brien, 2014; Sirenko *et al.*, 2015). In this study, we developed and validated a number of HCA-based assays and phenotypic read-outs, including characterizations of nuclear morphology, DNA content, cell cycle, cytoskeleton integrity and DNA damage responses using a germline cell line.

We selected the C18-4 germline cell line as an *in vitro* cell model to evaluate the testicular toxicity of BPA and its selected analogues (Hofmann *et al.*, 2005a,b; Kokkinaki *et al.*, 2009). Spermatogenesis is a complex process by which undifferentiated spermatogonial cells divide and mature, maintaining male fertility via the daily production of millions of spermatozoa in the testis. The foundation of this process lies in spermatogonial stem cells, which undergo self-renewal and produce daughter cells by undergoing complicated differentiation processes (Oatley and Brinster, 2008). The immortalized C18-4 germline cells exhibited the morphological features of spermatogonial cells and expressed germ cell-specific proteins (Hofmann *et al.*, 2005a). The C18-4 cells have been used to determine testicular signaling pathways (Golestaneh *et al.*, 2009; He *et al.*, 2008; Zhang *et al.*, 2013), and to characterize molecular mechanisms of reproductive toxicity of nanoparticles (Braydich-Stolle *et al.*, 2005, 2010; Lucas *et al.*, 2012). In combination with the validated

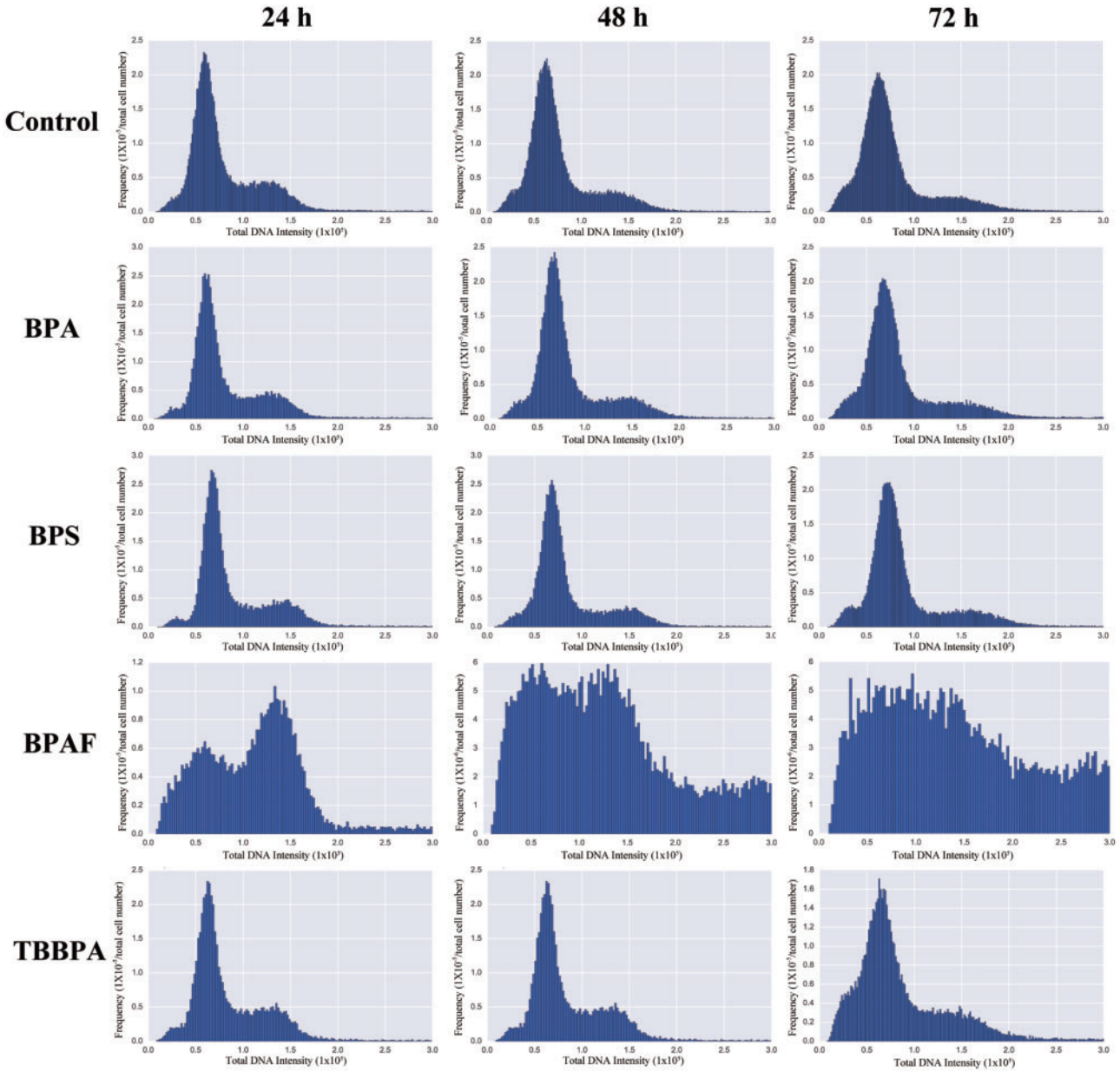

FIG. 6. HCA of cell cycle of spermatogonial cells treated with BPA, BPS, BPAF, and TBBPA. The representative DNA content histograms are shown in the controls (0.05% DMSO vehicle) and treatments with BPA and BPS (50 μM), BPAF and TBBPA (25 μM) for 24, 48, and 72 h.

HCA assays, we found this *in vitro* model suitable for quantitative screening of chemical effects in spermatogonial cells, enabling rapid and cost-effective assessment of reproductive toxicants.

Changes in nuclear morphology are general a reflection or a result of accumulation, of millions of cellular events taking place inside a cell, and known to be tightly associated with proliferation, gene expression, and protein synthesis (Versaevel *et al.*, 2012). Therefore, the nuclear morphology is a useful "readout" for toxicological assays. The nucleus is surrounded by the nuclear envelope, which isolates chromosomes from cytoplasm and typically has either an oval or round shape. Previous studies have demonstrated that the changes in nuclear morphology seen with HCA were sensitive markers for detecting cytotoxic effects (Martin *et al.*, 2014; O'Brien *et al.*, 2006; Persson *et al.*, 2013). In the present study, we found that BPA induced alterations of nuclear shape (LWR) at non-cytotoxic doses, which is similar to previous findings in mouse embryonic fibroblasts (Dolinoy *et al.*, 2007; Gassman *et al.*, 2016). An *in vivo* study recently demonstrated that low-dose exposure to BPA (2 μg/kg) induced germ cell apoptosis in adult rats (Jin *et al.*, 2013). Interestingly, we observed that BPAF induced a dose-dependent increase of multinucleated cells. Induction of abnormal testicular germ cells, such as multinucleated germ cells (MNGs), has been reported following gestational exposure to di-(n-butyl) phthalate (DBP) (Fisher *et al.*, 2003; Kleymenova *et al.*, 2005; Mahood *et al.*, 2007; Saffarini *et al.*, 2012). Ferrara and colleagues speculated that germ cells presenting DBP-induced MNGs may develop into carcinoma *in situ* cells, the known precursors of testicular germ cell tumors in men (Ferrara *et al.*, 2006). Cell cycle analysis revealed that these BPAF-induced multinucleated cells were actively synthesizing DNA (BrdU), with increased

TABLE 1. HCA of Cell Cycle of Spermatogonial Cells Treated with Various Concentrations of BPA, BPS, and BPAF, TBBPA for 24, 48, and 72 h

	Dose (μM)	24 h				48 h				72 h			
		Sub G1(%)[a]	G0/1(%)	S (%)	G2/M (%)	Sub G1(%)[a]	G0/1(%)	S (%)	G2/M (%)	Sub G1(%)[a]	G0/1(%)	(%)S	G2/M (%)
BPA	0	3.5 ± 1.1	64.6 ± 1.7	12.6 ± 0.8	18.1 ± 1.7	5.2 ± 1.5	67.4 ± 1.6	12.0 ± 0.7	13.0 ± 1.1	5.6 ± 1.0	70.7 ± 1.7	9.9 ± 1.4	12.9 ± 1.0
	0.1	3.5 ± 0.9	64.9 ± 1.5	12.6 ± 0.2	18.1 ± 1.1	5.2 ± 3.1	69.4 ± 2.3	12.4 ± 0.7	12.5 ± 2.8	6.9 ± 1.2	70.0 ± 0.8	10.6 ± 0.6	11.7 ± 1.3
	1	4.4 ± 2.1	62.5 ± 1.5	12.9 ± 0.8	18.9 ± 1.9	5.9 ± 1.5	67.9 ± 1.2	12.1 ± 0.6	13.6 ± 1.8	6.5 ± 1.1	70.7 ± 2.1	9.3 ± 2.1	12.2 ± 1.0
	10	5.0 ± 1.3	64.0 ± 1.0	11.8 ± 0.9	18.3 ± 1.3	4.7 ± 1.4	67.0 ± 2.2	11.7 ± 1.4	15.7 ± 1.2*	6.8 ± 0.6	70.6 ± 3.1	11.3 ± 2.6	9.8 ± 1.2*
	50	4 ± 1.3	65.8 ± 3.0	13.5 ± 0.6	15.3 ± 1.3*	4.2 ± 1.7	67.1 ± 1.9	12.9 ± 0.8	15.1 ± 1.6	7.3 ± 1.3*	67.5 ± 3.1	11.0 ± 1.7	13.1 ± 1.9
BPS	0	3.5 ± 1.1	64.6 ± 1.7	12.6 ± 0.8	18.1 ± 1.7	5.2 ± 1.5	67.4 ± 1.6	12.0 ± 0.7	13.0 ± 1.1	5.6 ± 1.0	70.7 ± 1.7	9.9 ± 1.4	12.9 ± 1
	0.1	3.8 ± 0.8	63.6 ± 1.5	12.3 ± 0.2	19.4 ± 2.0	4.3 ± 0.6	69.5 ± 1.1	11.8 ± 0.7	13.7 ± 1.8	7.4 ± 1.7	71.0 ± 1.1	9.5 ± 1.3	11.4 ± 0.8
	1	3.6 ± 0.7	62.9 ± 2.0	12.6 ± 0.5	20.0 ± 1.1	3.7 ± 1.8	68.4 ± 1.8	11.7 ± 0.5	15.0 ± 1.6	6.5 ± 0.6	71.9 ± 1.8	9.6 ± 1.4	11.3 ± 1.1
	10	3.8 ± 0.9	63.1 ± 1.9	12.9 ± 0.7	19.2 ± 1.3	4.9 ± 1.3	66.6 ± 1.2	11.9 ± 0.9	15.6 ± 2.3*	8.7 ± 5.0	70.1 ± 1.9	10.2 ± 1.5	10.2 ± 2.8*
	50	3.9 ± 1.1	63.7 ± 1.3	13.0 ± 0.8	18.6 ± 1.6	5.9 ± 3.4	65.9 ± 2.5	11.2 ± 0.9	16.0 ± 1.9*	7.4 ± 1.4	70.5 ± 2.5	9.2 ± 1.6	11.8 ± 2.6
BPAF	0	3.5 ± 1.1	64.6 ± 1.7	12.6 ± 0.8	18.1 ± 1.7	5.2 ± 1.5	67.4 ± 1.6	12.0 ± 0.7	13.0 ± 1.1	5.6 ± 1.0	70.7 ± 1.7	9.9 ± 1.4	12.9 ± 1.0
	0.1	3.6 ± 1.0	64.3 ± 1.9	11.9 ± 1.0	18.5 ± 1.3	5.6 ± 1.9	66.5 ± 2.2	10.6 ± 0.4	16.6 ± 1.4	6.5 ± 0.7	71.5 ± 1.0	10.4 ± 0.5	11.1 ± 1.1
	1	3.3 ± 0.7	65.1 ± 1.4	13.5 ± 0.5	17.3 ± 2.0	5.4 ± 1.4	68.1 ± 2.0	11.5 ± 1.4	14.0 ± 2.1	7.7 ± 1.1	67.9 ± 3.3	10.9 ± 1.1	12.8 ± 1.2
	5	4.1 ± 1.0	63.5 ± 2.8	12.1 ± 0.7	18.7 ± 1.5	5.5 ± 2.0	67.8 ± 3.5	11.6 ± 1.3	14.1 ± 4.2	8.0 ± 0.7*	70.0 ± 1.0	10.3 ± 1.2	11.2 ± 1.1
	10	6.1 ± 1.6*	62.2 ± 1.8	12.3 ± 0.8	18.5 ± 1.2	8.4 ± 4.1	59.7 ± 1.5*	11.0 ± 0.6	19.9 ± 3.2*	12.1 ± 2.5*	61.0 ± 1.3*	13.1 ± 2.1*	13.1 ± 1.1
	25	7.6 ± 1.9*	25.3 ± 3.3*	14.9 ± 1.6*	47.6 ± 4.6*	9.7 ± 1.7*	25.3 ± 3.1*	15.2 ± 1.4*	44.6 ± 2.7*	6.8 ± 2.5	26.4 ± 3.0*	19.3 ± 1.3*	48.3 ± 5.1*
TBBPA	0	3.5 ± 1.1	64.6 ± 1.7	12.6 ± 0.8	18.1 ± 1.7	5.2 ± 1.5	67.4 ± 1.6	12.0 ± 0.7	13.0 ± 1.1	5.6 ± 1.0	70.7 ± 1.7	9.9 ± 1.4	12.9 ± 1.0
	0.1	4.9 ± 2.0	62.4 ± 1.7	12.9 ± 0.7	19.1 ± 2.0	4.1 ± 1.9	69.1 ± 1.9	11.4 ± 0.4	14.8 ± 3.3	7.4 ± 1.2	71.0 ± 0.5	10.3 ± 0.4	10.8 ± 0.9
	1	3.7 ± 1.0	62.7 ± 1.0	13.3 ± 0.8	19.6 ± 1.1	5.4 ± 1.4	66.7 ± 2.8	12.0 ± 0.8	15.0 ± 2.9	8.6 ± 0.9	69.4 ± 0.7	10.5 ± 0.5	10.6 ± 0.7
	5	4.3 ± 1.5	62.9 ± 1.7	13.2 ± 0.7	18.7 ± 0.9	3.4 ± 1.1	67.6 ± 1.6	11.9 ± 0.6	16.3 ± 2.0*	8.6 ± 4.5	69.7 ± 3.7	9.9 ± 0.4	11.2 ± 0.7
	10	4.2 ± 1.5	66.3 ± 1.7	11.0 ± 1.1*	18.0 ± 2.1	5.5 ± 1.7	66.5 ± 1.6	8.9 ± 2.3*	18.1 ± 1.4*	11.0 ± 2.0*	67.7 ± 1.6	6.7 ± 0.6*	13.8 ± 1.0
	25	4.7 ± 1.0	60.3 ± 0.9*	10.6 ± 1.2*	23.5 ± 0.9*	8.9 ± 3.6*	63.2 ± 3.3*	9.2 ± 1.3*	17.7 ± 2.0*	13.2 ± 2.3*	57.5 ± 8.0*	8.7 ± 1.1	19.1 ± 4.9*

Note: Percentage of each stage of cell cycle, including sub-G1, G0/1, S and G2/M phase are presented as mean ± SD, $n = 6$. Three replicates in 2 separate experiments were included. Statistical analysis was conducted by 1-way ANOVA followed by Tukey-Kramer multiple comparison (*$P < .05$). Cells treated with vehicle (0.05% DMSO) were used as negative controls (0).

[a]Cells with DNA content less than 2N, representing apoptotic cells.

numbers of cells in S and G2/M phase, suggesting these germline cells underwent abnormal proliferation. Further animal studies are need to confirm whether BPAF has a testicular toxicity similar to DBP *in vivo*.

Assessment of the cell cycle status of individual cells is pivotal for the evaluation of cell cycle regulation in response to intracellular and extracellular cues. Cell cycle status and progression has traditionally been measured using population-based methods such as flow cytometry (Darzynkiewicz *et al.*, 2006; Sidhu *et al.*, 2006). Flow cytometry is generally dependent on the successful preparation of a single-cell suspension, which is not compatible with high-throughput and high-resolution cell imaging. HCA-based cell cycle analysis was recently reported by Roukos *et al.* (2015). Cell cycle profiles with discrete G1, S or G2/M populations were determined and these results were comparable to data obtained from flow cytometry analysis (Roukos *et al.*, 2015). We have established a protocol for the spermatogonial cell line, which was able to accurately segment the nuclei for DNA content quantification. We have shown the dynamic changes of the cell cycle in the control population at different time-points (Table 1). Those percentage changes across the phases of the cell cycle are consistent with the cellular growth status, exhibiting fast proliferation at an early time-point and then slowing down when cells reach 100% confluence for 72 h. This HCA-based cell cycle analysis allows us to be able to accurately segment the nuclei even when the C18-4 spermatogonial cells were at 100% confluence for 72 h. As an imaging-based method to probe the cell cycle phase of individual cells, HCA can be used to correlate phases with the subcellular localization or the co-expression levels of multiple DNA loci or proteins tagged with different fluorescent markers. This feature will be widely applied in the mechanistic toxicity studies to screen or identify potential mechanisms of action. As revealed in the cell cycle analysis using HCA-based DNA content histograms and BrdU incorporation assay, we found that BPA and its analogues induced dose- and time-dependent alterations of the cell cycle with chemical specific changes. Previous *in vivo* studies showed that BPA disrupted meiosis I progression and altered the number of leptotene and diplotene spermatocytes percentages in rat testicular cells (Ali *et al.*, 2014; Liu *et al.*, 2013). Disruption of the cell cycle has been proposed to be a key event in BPA testicular toxicity (Ali *et al.*, 2014; Liu *et al.*, 2013). Our results demonstrated that BPA or BPS treatments at a concentration of 10 or 50 μM disrupted mitosis progression (G2/M phase). BPA induced dose-dependent decrease of BrdU positive cells for 48 h, suggesting that HCA-based quantification of BrdU is a sensitive endpoint for the evaluation of the cell cycle on comparison to the cell cycle profiling from total DNA content histogram. It has been reported that BPA exposure caused diverse effects on the cell cycle. BPA treatment can inhibit cell proliferation and induced S and G2/M phase arrest in midbrain cells at 1×10^{-4} M (Liu *et al.*, 2013). On the other side, low-dose BPA ($\leq 10^{-9}$ M) can promote cell proliferation in human seminoma cells though a G-protein-coupled non-classical membrane estrogen receptor (ER) and induced cell proliferation and cell-cycle regulatory proteins in human breast cell lines (Bouskine *et al.*, 2009; Pfeifer *et al.*, 2015; Wu *et al.*, 2012). The differences between our current observations and previous studies may be due to the different sensitivity to the endpoints tested in spermatogonial cells. For BPAF treatment, along with the significant changes of nuclear morphology, we observed significant increases of S phase in both cell cycle profiling and BrdU labeling, and

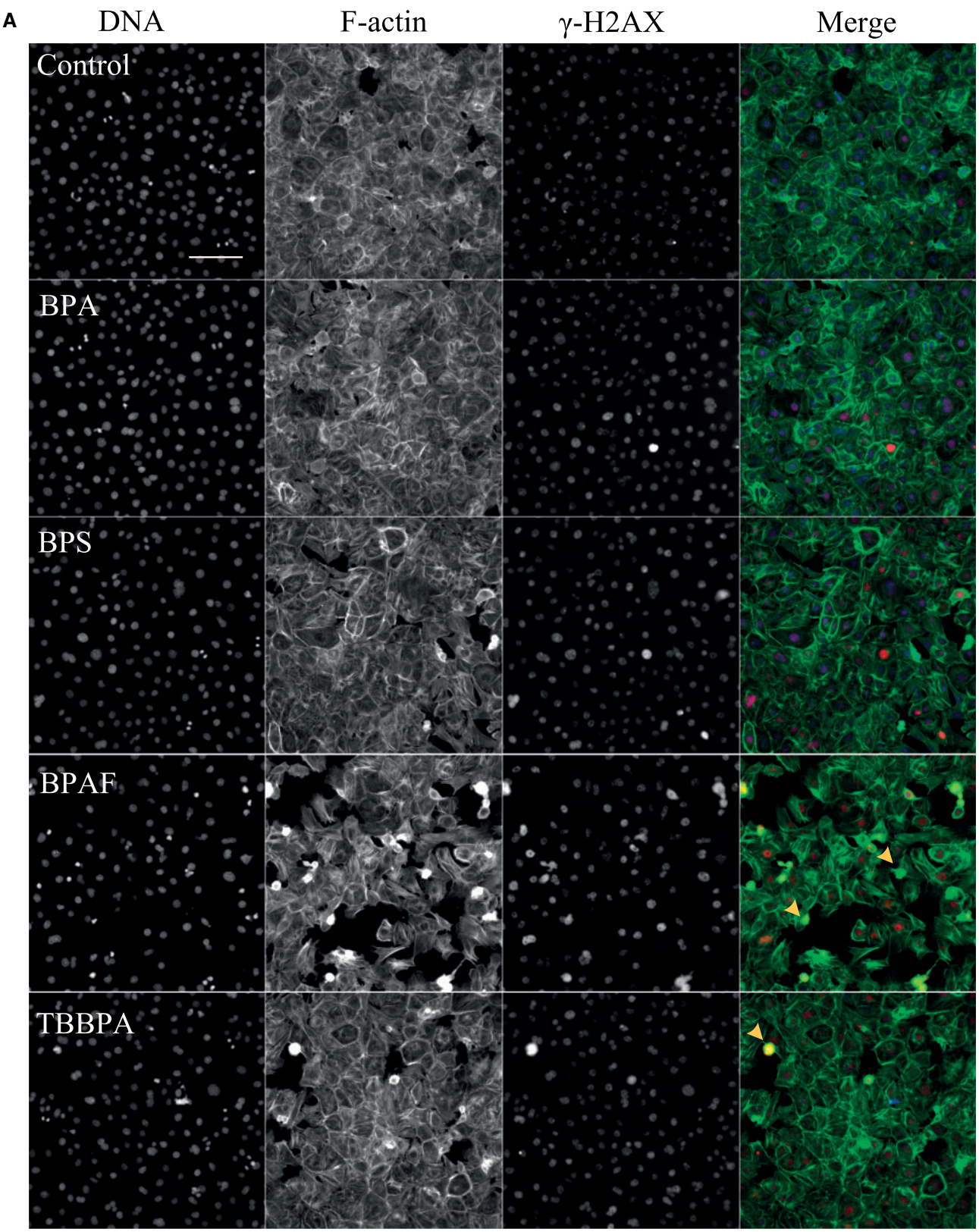

FIG. 7. HCA of F-actin and γ-H2AX in spermatogonial cells treated with BPA, BPS, BPAF, and TBBPA. Cells were treated with various concentrations of BPA and BPS (0.1, 1, 10, and 50 μM), and BPAF and TBBPA (0.1, 1, 5, 10, and 25 μM) for 24, 48, and 72 h. Cells treated with vehicle (0.05% DMSO) were used as negative controls (0). The nuclei were stained with Hoechst 33342 (blue), F-actin with Phalloidin staining (green), and γ-H2AX with combination of primary anti-γ−H2AX and secondary Dylight 650 conjugated antibody (red). A shows the representative images of cells treated with BPA and BPS (50 μM), BPAF and TBBPA (25 μM) for 24 h. Arrows indicate dot-like structures. Scale bar = 100 μm. B-C demonstrated the quantification of log-transformed total intensity of F-actin and positive γ-H2AX cells. Data were presented as mean ± SD, $n = 6$. Three replicates in 2 separate experiments were included. Statistical analysis was conducted by 1-way ANOVA followed by Tukey-Kramer multiple comparison (*$P < .05$).

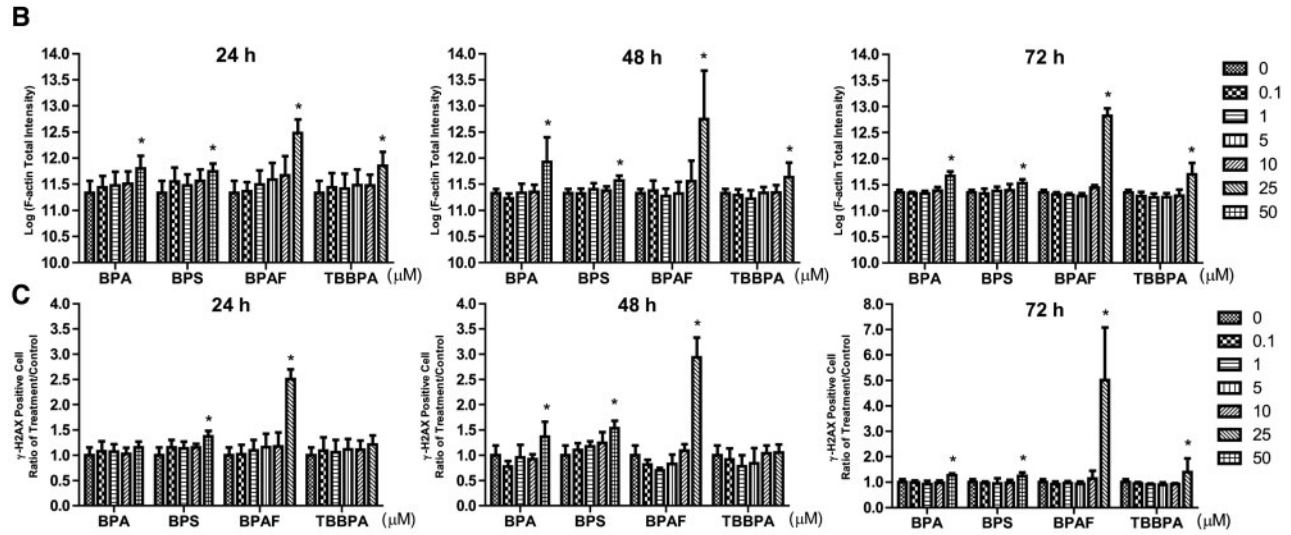

FIG. 7. Continued.

TABLE 2. Correlation Analysis Between Total Intensity of F-actin and Total Intensity of γ-H2AX

	Correlation Coefficient									
Time (h)	BPA		BPS		BPAF		TBBPA		All	
	r	*P*	*r*	*P*	*r*	*P*	*r*	*P*	*r*	*P*
24	0.85	<.0001	0.91	<.0001	0.45	.0384	0.75	<.0001	0.76	<.0001
48	0.82	<.0001	0.89	<.0001	0.74	.0001	0.34	.1295	0.75	<.0001
72	0.42	.0827	0.66	.0027	0.48	.0276	0.52	.0152	0.50	<.0001

Note: Spearman correlation analysis was conducted between the log-transformed total intensity of F-actin and γ-H2AX in each cell (JMP statistical analysis package, SAS Institute, Cary, North Carolina).

accumulation of cells in G2/M phase in a dose-dependent manner. Again, HCA-based assessment of the cell cycle status of individual cells suggested that BPAF treatment could result in significant alterations of cell cycle as compared with the treatment with BPA, BPS, or TBBPA at similar dose ranges.

BPA has long been suspected to induce carcinogenesis (Keri *et al.*, 2007). Low doses of BPA have been reported to promote DNA damage, potentially contributing to breast cancer (Pfeifer *et al.*, 2015). Several assays can measure and quantify cellular responses to DNA double-strand breaks. The proteins, such as γ-H2AX, ATM, CDKN1A, and TP53, involved in the early steps of the cellular response in sensing DNA damage and controlling progression, have been proposed as the top group of candidate biomarkers (Marchetti *et al.*, 2006). Due to the signal amplification of γ-H2AX foci at the site of DNA damage, the detection of γ-H2AX has been identified as an early sensitive cellular biomarker of DNA damage (Nikolova *et al.*, 2014; Rogakou *et al.*, 1998). In this study, we developed a multi-parametric HCA assay along with the detection of γ-H2AX and found that BPA and its analogues significantly altered the expression levels of γ-H2AX. It has been reported that BPA and its analogues induced DNA damages in a cell-type-specific and dose-dependent manner (Fic *et al.*, 2013; Lee *et al.*, 2013). BPA is able to induce DNA damage in spermatozoa (Liu *et al.*, 2013), and in human breast cell line MCF-7 cells at the low concentration of 10 nM (Liu *et al.*, 2013; Pfeifer *et al.*, 2015). Other studies showed that BPA at concentration of 100 μM did not induce γ-H2AX in a colorectal adenocarcinoma LSI174T cell line, but Bisphenol F did (Audebert *et al.*, 2011). Most significantly, among all chemicals tested, BPAF showed significant induction of γ-H2AX at multiple timepoints, suggesting a greater genotoxicity, as compared with other bisphenols.

The cytoskeleton, which serves as a scaffold that determines cell shape and the organization of the cytoplasm, plays a significant role in regulating cell shape, movement, cargo transportation and nuclear morphological modification (Sun *et al.*, 2011). Disorganization of F-actin was found to induce germ cells dysfunction *in vivo* (Lie *et al.*, 2009). A BPA exposure of 200 μM induced the truncation and depolymerization of F-actin with mislocalization of actin regulatory proteins in human Sertoli cells without the changes of the total F-actin fluorescence intensity (Xiao *et al.*, 2014). HCA-based analysis of F-actin demonstrated that all 4 bisphenols showed aberrant F-actin distribution in the cytoplasm (Figure 7B). These alterations in F-actin are highly correlated with the increased γ-H2AX expression, an early DNA damage responses marker (Table 3). It has been reported that alterations in the actin cytoskeleton were correlated with induction of γ-H2AX in human breast MCF-7 cells (Zhao *et al.*, 2015). In this study, comparison of EC20 values indicated F-actin appeared an early cellular response marker for chemical-induced testicular toxicity, and that perturbation of the cytoskeleton could potentially be associated with other endpoints, such as change of nuclear morphology and cell cycle alterations.

One of the applications of HCA assays in drug discovery and toxicity testing is prioritizing and ranking compounds for their potential human toxicity. By comparing of EC20 values among 4 bisphenols, BPAF showed the highest germ cell cytotoxicity, followed by TBBPA, BPA, and BPS. Although the chemical structures of BPA and its analogues are similar, HCA demonstrated differential adverse effects of 4 bisphenols on multiple molecular and cellular events, suggesting that different mechanisms may promote cytotoxicity. Similar findings were reported in previous *in vitro* studies, in which BPAF and TBBPA showed higher endocrine modulating potentials in human MCF7 breast

TABLE 3. EC_{20} Values of BPA and Its Selected Analogues from Multiple Endpoints

		24 h				48 h				72 h			
	Dose (μM)	BPA	BPS	BPAF	TBBPA	BPA	BPS	BPAF	TBBPA	BPA	BPS	BPAF	TBBPA
Cell Viability [a]	EC_{20}	114.5	4222.1	11.5	41.7	84	154.3	10.1	47.1	ND			
	CI	101.1–129.6	198.6–248.3	3.9–33.4	31.5–55.2	72.8–97.0	123.1–193.4	39.6–25.7	VW				
Cell Number	EC_{20}	52.4	246.1	13.3	27.8	50	81.4	13.9	28.1	52.5	64.8	15.7	23.6
	CI	26.1–105.4	26.2–2316	11.0–16.0	17.9–43.0	VW	36.6–180.8	11.6–16.6	21.4–36.9	47.7–57.9	47.9–87.7	13.9–17.6	21.8–25.5
Nuclear Area	EC_{20}	NS	NS	20.8	NS	NS	NS	18.1	NS	NS	108.1	12.5	26.4
	CI			VW				VW			54.3–215	VW	VW
P2A	EC_{20}	NS	NS	8.7	NS	NS	NS	8.3	NS	NS	—	7.7	33.8
	CI			7.8–9.9				7.4–9.2			—	6.5–9.1	25.8–44.3
LWR	EC_{20}	NS	NS	6.8	NS	NS	NS	7.6	NS	70.9	61.8	6.1	11.8
	CI			3.5–13.0				5.7–10.0		32.5–154.3	35.3–108.2	5.3–7.1	5.7–24.4
Cell Cycle (Sub G1)	EC_{20}	NS	NS	5.8	NS	NS	NS	6.3	13.7	—	NS	0.4	0.3
	CI			3.6–9.2				2.9–13.5	4.7–40.0	—		0.03–4.2	0.05–1.6
Cell Cycle (G0/1)	EC_{20}	NS	NS	11.4	—	NS	NS	10.1	38.0	NS	NS	9.8	18.9
	CI			6.1–21.3	—			VW	20.6–70.0			9.4–10.2	15.8–22.5
Cell Cycle (S)	EC_{20}	NS	NS	19.3	8.8	NS	NS	17.12	5.7	NS	NS	8.6	23.5
	CI			VW	VW			VW	VW			7.0–10.1	9.0–62.1
Cell Cycle (G2/M)	EC_{20}	54.6	NS	11.9	25.2	NS	—	9.8	52.2	NS	NS	12.0	24.7
	CI	VW		VW	VW		—	9.2–10.5	13.8–198.1			VW	21.7–28.1
BrdU	EC_{20}	NS	36.9	10.7	NS	—	78	10.4	NS	NS	NS	12.2	NS
	CI		15.8–86.2	8.6–13.3		—	12.9–472.4	VW				18.3–81.8	
γ-H2AX	EC_{20}	NS	31.0	10.9	NS	50.3	20.6	11.2	NS	60.2	56.6	11.3	26.1
	CI		9.5–101.1	8.7–13.7		VW	9.9–42.9	VW		VW	VW	VW	
F-actin	EC_{20}	7.5	4.5	7.8	10.1	31.5	66.2	10.2	24.4	47.0	99.4	10.9	24.6
	CI	1.7–34.0	0.7–28.6	5.5–11.1	5.8–20.5	12.4–80.0	36.2–121.1	VW	20.1–28.4	41.1–53.8	39.2–252.1	VW	VW

Notes. EC_{20}: Values for does causing 20% of the maximum response. CI: 95% confidence interval. NS: not significant. ND: not determined. VW: very wide; —, EC_{20} simulation failed (exceeded treatment concentration that decreased cell viability to 0%). Color code: red, increase; green, decrease.

[a]Data from NR uptake assay.

cancer cells and Leydig cells, respectively, as compared with BPA (Lei *et al*., 2016; Roelofs *et al*., 2015). BPS showed similar inhibitory effects with BPA on testosterone secretion in human fetal testes and induced more sensitive responses in mice testes (Eladak *et al*., 2015). The different levels of toxicities between BPA and its analogues could be dependent on their chemical structures. Perez *et al.* (1998) reported that the estrogenicity of BPA analogues in human breast cancer cells was influenced by the substitution at the bridging carbon between the 2 phenolic rings in human breast cancer cells. In addition, for BPAF and TBBPA, introducing a halogen into the bisphenol structure could contribute to their higher toxicities. This is because the degree of halogenation in BPA analogues could alter activation of ERs and peroxisome proliferator–activated receptors (PPARs) (Riu *et al*., 2011). By substituting different chemical groups and degree of halogenation, BPA and its analogues could exert differential toxicities via various receptor binding sites and binding affinities. In order to elucidate the potential structure-related toxicities, more BPA analogues will be included in future studies. Our *in vitro* data were also consistent with previous *in vivo* findings. BPA exposure ($\leq$50 mg/kg) consistently induced impairments of sperm production and quality, and alteration of steroidogenesis (D'Cruz *et al*., 2012; Tiwari and Vanage, 2013). Whereas BPS, BPAF, and TBBPA exerted some adverse reproductive effects, including alterations of hormone levels, decreases in sperm count and changes of seminiferous epithelium morphology, Future study will be important to validate these findings (Feng *et al*., 2012; Kuriyama *et al*., 2005; Ullah *et al*., 2016).

Several limitations of the *in vitro* HCA assay need to be considered. First, bioactivation might be required, but it is limited in our current *in vitro* cell culture model. It has been reported that metabolites of BPA, such as 4-methyl-2, 4-bis (p-hydroxyphenyl) pent-1-ene, exhibited higher estrogenic potency as compared with BPA itself (Yoshihara *et al*., 2004). Thus metabolites of BPA and its analogues should be included in further experiments. Second, the duration of exposure might be insufficient. In order to mimic real-life exposure scenarios, chronic low-dose exposure to BPA and its analogues need to be considered. Third, the species-specific sensitivity for *in vitro* testing is critical to the interpretation of toxicity across species. It has been reported that BPA concentration required to impair testosterone production in human is about 100-fold lower than that in rodent fetal testis explants (Habert *et al*., 2014). Thus, more cell lines or primary cells from different species, especially humans, would be helpful to extrapolate current *in vitro* findings to human health risk assessment.

In summary, we have developed multi-parametric HCA assays in germline cells and compared the testicular toxicity of BPA to some of its analogues. This multi-dimensional toxicological profiling revealed differential testicular toxicities of BPA and its analogues, whereas BPAF and TBBPA showed greater cytotoxicity, followed by BPA and BPS. Our findings also suggested that using the HCA platform with C18-4 spermatogonial cells could provide a rapid and cost-efficient tool to gain insights into mechanisms of toxicity, and establish links between molecular pathways and accelerate safety testing of potential reproductive toxicants.

SUPPLEMENTARY DATA

Supplementary data are available online at http://toxsci.oxfordjournals.org/.

ACKNOWLEDGMENTS

We thank Mr Jake Maas for proofreading the manuscript.

FUNDING

This work was supported by the Centers for Disease Control and Prevention, The National Institute for Occupational Safety and Health (NIOSH) under award number R21 OH 010473; National Institute of Environmental Health Sciences of the National Institutes of Health under award number R43ES027374; Alternatives Research & Development Foundation (ARDF) and University of Georgia Startup Research funding (1025AR715005).

REFERENCES

Ali, S., Steinmetz, G., Montillet, G., Perrard, M. H., Loundou, A., Durand, P., Guichaoua, M. R., and Prat, O. (2014). Exposure to low-dose bisphenol A impairs meiosis in the rat seminiferous tubule culture model: a physiotoxicogenomic approach. *PloS One* **9**, e106245. 10.1371/journal.pone.0106245.

Anguissola, S., Garry, D., Salvati, A., O'Brien, P. J., and Dawson, K. A. (2014). High content analysis provides mechanistic insights on the pathways of toxicity induced by amine-modified polystyrene nanoparticles. *PloS One* **9**, 10.1371/journal.pone.0108025.

Ankley, G. T., Bennett, R. S., Erickson, R. J., Hoff, D. J., Hornung, M. W., Johnson, R. D., Mount, D. R., Nichols, J. W., Russom, C. L., Schmieder, P. K., *et al.* (2010). Adverse outcome pathways: a conceptual framework to support ecotoxicology research and risk assessment. *Environ. Toxicol. Chem.* **29**, 730–741. 10.1002/etc.34.

Audebert, M., Dolo, L., Perdu, E., Cravedi, J. P., and Zalko, D. (2011). Use of the gamma H2AX assay for assessing the genotoxicity of bisphenol A and bisphenol F in human cell lines. *Arch. Toxicol.* **85**, 1463–1473. 10.1007/s00204-011-0721-2.

Auerbach, S., Filer, D., Reif, D., Walker, V., Holloway, A. C., Schlezinger, J., Srinivasan, S., Svoboda, D., Judson, R., Bucher, J. R., *et al.* (2016). Prioritizing environmental chemicals for obesity and diabetes outcomes research: a screening approach using toxcast high throughput data. *Environ. Health Perspect.* **124**, 1141–1154. doi: 10.1289/ehp.1510456, 10.1289/ehp.1510456.

Bouskine, A., Nebout, M., Brucker-Davis, F., Benahmed, M., and Fenichel, P. (2009). Low doses of bisphenol a promote human seminoma cell proliferation by activating PKA and PKG via a membrane G-protein-coupled estrogen receptor. *Environ. Health Persp.* **117**, 1053–1058.

Braun, J. M., Kalkbrenner, A. E., Calafat, A. M., Yolton, K., Ye, X. Y., Dietrich, K. N., and Lanphear, B. P. (2011). Impact of early-life bisphenol A exposure on behavior and executive function in children. *Pediatrics* **128**, 873–882. 10.1542/peds.2011-1335.

Braydich-Stolle, L., Hussain, S., Schlager, J. J., and Hofmann, M. C. (2005). In vitro cytotoxicity of nanoparticles in mammalian germline stem cells. *Toxicological Sciences* **88**, 412–419.

Braydich-Stolle, L. K., Lucas, B., Schrand, A., Murdock, R. C., Lee, T., Schlager, J. J., Hussain, S. M., and Hofmann, M. C. (2010). Silver nanoparticles disrupt GDNF/Fyn kinase signaling in spermatogonial stem cells. *Toxicol. Sci.* **116**, 577–589. 10.1093/toxsci/kfq148.

Calafat, A. M., Kuklenyik, Z., Reidy, J. A., Caudill, S. P., Ekong, J., and Needham, L. L. (2005). Urinary concentrations of

bisphenol A and 4-nonylphenol in a human reference population. *Environ. Health Persp.* **113**, 391–395.

Calafat, A. M., Ye, X. Y., Wong, L. Y., Reidy, J. A., and Needham, L. L. (2008). Exposure of the US population to bisphenol A and 4-tertiary-octylphenol: 2003-2004. *Environ. Health Persp.* **116**, 39–44.

Carwile, J. L., and Michels, K. B. (2011). Urinary bisphenol A and obesity: NHANES 2003-2006. *Environ. Res.* **111**, 825–830. 10.1016/j.envres.2011.05.014.

Chen, D., Kannan, K., Tan, H. L., Zheng, Z. G., Feng, Y. L., Wu, Y., and Widelka, M. (2016). Bisphenol analogues other than BPA: environmental occurrence, human exposure, and toxicity-A review. *Environ. Sci. Technol.* **50**, 5438–5453. 10.1021/acs.est.5b05387.

Colnot, T., Kacew, S., and Dekant, W. (2014). Mammalian toxicology and human exposures to the flame retardant 2,2',6,6'-tetrabromo-4,4'-isopropylidenediphenol (TBBPA): implications for risk assessment. *Arch. Toxicol.* **88**, 553–573. 10.1007/s00204-013-1180-8.

D'Cruz, S. C., Jubendradass, R., Jayakanthan, M., Rani, S. J. A., and Mathur, P. P. (2012). Bisphenol A impairs insulin signaling and glucose homeostasis and decreases steroidogenesis in rat testis: An in vivo and in silico study. *Food Chem Toxicol.* **50**, 1124–1133. 10.1016/j.fct.2011.11.041.

Darzynkiewicz, Z., Huang, X., and Okafuji, M. (2006). Detection of DNA strand breaks by flow and laser scanning cytometry in studies of apoptosis and cell proliferation (DNA replication). *Methods Mol. Biol.* **314**, 81–93.

Dolinoy, D. C., Huang, D., and Jirtle, R. L. (2007). Maternal nutrient supplementation counteracts bisphenol A-induced DNA hypomethylation in early development. *Proc. Natl. Acad. Sci. USA* **104**, 13056–13061. 10.1073/pnas.0703739104.

Ehrlich, S., Williams, P. L., Missmer, S. A., Flaws, J. A., Berry, K. F., Calafat, A. M., Ye, X. Y., Petrozza, J. C., Wright, D., and Hauser, R. (2012). Urinary Bisphenol A Concentrations and implantation failure among women undergoing in vitro fertilization. *Environ. Health Persp.* **120**, 978–983.

Eladak, S., Grisin, T., Moison, D., Guerquin, M. J., N'Tumba-Byn, T., Pozzi-Gaudin, S., Benachi, A., Livera, G., Rouiller-Fabre, V., and Habert, R. (2015). A new chapter in the bisphenol A story: bisphenol S and bisphenol F are not safe alternatives to this compound. *Fert. Ster.* **103**, 11–21.

Elmore, S. (2007). Apoptosis: A review of programmed cell death. *Toxicol. Pathol.* **35**, 495–516.

FDA. (2012). *Indirect Food Additives: Polymers*. In: Vol. 21 CFR 177, pp. 41899–41902.

FDA. (2013). *Indirect Food Additives: Adhesives and Components of Coatings*. In: Vol. 21 CFR 175, pp. 41840–41843.

Feng, Y. X., Yin, J., Jiao, Z. H., Shi, J. C., Li, M., and Shao, B. (2012). Bisphenol AF may cause testosterone reduction by directly affecting testis function in adult male rats. *Toxicol. Lett.* **211**, 201–209.

Ferrara, D., Hallmark, N., Scott, H., Brown, R., McKinnell, C., Mahood, I. K., and Sharpe, R. M. (2006). Acute and long-term effects of in utero exposure of rats to di(n-butyl) phthalate on testicular germ cell development and proliferation. *Endocrinology* **147**, 5352–5362. 10.1210/en.2006-0527.

Fic, A., Zegura, B., Dolenc, M. S., Filipic, M., and Masic, L. P. (2013). Mutagenicity and DNA damage of bisphenol a and its structural analogues in Hepg2 cells. *Arh Hig Rada Toksiko* **64**, 189–200. 10.2478/10004-1254-64-2013-2319.

Fisher, J. S., Macpherson, S., Marchetti, N., and Sharpe, R. M. (2003). Human 'testicular dysgenesis syndrome': a possible model using in-utero exposure of the rat to dibutyl phthalate. *Hum. Reprod.* **18**, 1383–1394.

Gassman, N. R., Coskun, E., Jaruga, P., Dizdaroglu, M., and Wilson, S. H. (2016). Combined effects of high-dose bisphenol A and oxidizing agent (KBrO) on cellular microenvironment, gene expression, and chromatin structure of Ku70-deficient mouse embryonic fibroblasts. *Environ. Health Perspect.* **124**, 1241–1252. doi: 10.1289/EHP237, 10.1289/EHP237.

Golestaneh, N., Beauchamp, E., Fallen, S., Kokkinaki, M., Uren, A., and Dym, M. (2009). Wnt signaling promotes proliferation and stemness regulation of spermatogonial stem/progenitor cells. *Reproduction* **138**, 151–162.

Habert, R., Muczynski, V., Grisin, T., Moison, D., Messiaen, S., Frydman, R., Benachi, A., Delbes, G., Lambrot, R., Lehraiki, A., *et al.* (2014). Concerns about the widespread use of rodent models for human risk assessments of endocrine disruptors. *Reproduction* **147**, R119–R129.

Harris, S., Hermsen, S. A. B., Yu, X. Z., Hong, S. W., and Faustman, E. M. (2015). Comparison of toxicogenomic responses to phthalate ester exposure in an organotypic testis co-culture model and responses observed in vivo. *Reprod. Toxicol.* **58**, 149–159. 10.1016/j.reprotox.2015.10.002.

He, Z. P., Jiang, J. J., Kokkinaki, M., Golestaneh, N., Hofmann, M. C., and Dym, M. (2008). GDNF upregulates c-fos transcription via the Ras/ERK1/2 pathway to promote mouse spermatogonial stem cell proliferation. *Stem Cells* **26**, 266–278. 10.1634/stemcells.2007-0436.

Hofmann, M. C., Braydich-Stolle, L., Dettin, L., Johnson, E., and Dym, M. (2005a). Immortalization of mouse germ line stem cells. *Stem Cells* **23**, 200–210. 10.1634/stemcells.2003-0036.

Hofmann, M. C., Braydich-Stolle, L., and Dym, M. (2005b). Isolation of male germ-line stem cells; influence of GDNF. *Dev. Biol.* **279**, 114–124. 10.1016/j.ydbio.2004.12.006.

Jin, P., Wang, X., Chang, F., Bai, Y., Li, Y., Zhou, R., and Chen, L. (2013). Low dose bisphenol A impairs spermatogenesis by suppressing reproductive hormone production and promoting germ cell apoptosis in adult rats. *J. Biomed. Res.* **27**, 135–144. 10.7555/JBR.27.20120076.

Kameoka, S., Babiarz, J., Kolaja, K., and Chiao, E. (2014). A high-throughput screen for teratogens using human pluripotent stem cells. *Toxicol. Sci.* **137**, 76–90. 10.1093/toxsci/kft239.

Kang, J. H., Kondo, F., and Katayama, Y. (2006). Human exposure to bisphenol A. *Toxicology* **226**, 79–89. 10.1016/j.tox.2006.06.009.

Karmaus, A. L., Filer, D. L., Martin, M. T., and Houck, K. A. (2016). Evaluation of food-relevant chemicals in the ToxCast high-throughput screening program. *Food Chem. Toxicol.* **92**, 188–196. 10.1016/j.fct.2016.04.012.

Kavlock, R., Chandler, K., Houck, K., Hunter, S., Judson, R., Kleinstreuer, N., Knudsen, T., Martin, M., Padilla, S., Reif, D., *et al.* (2012). Update on EPA's toxcast program: providing high throughput decision support tools for chemical risk management. *Chem. Res. Toxicol.* **25**, 1287–1302.

Keri, R. A., Ho, S. M., Hunt, P. A., Knudsen, K. E., Soto, A. M., and Prins, G. S. (2007). An evaluation of evidence for the carcinogenic activity of bisphenol A. *Reprod. Toxicol.* **24**, 240–252. 10.1016/j.reprotox.2007.06.008.

Kitamura, S., Suzuki, T., Sanoh, S., Kohta, R., Jinno, N., Sugihara, K., Yoshihara, S., Fujimoto, N., Watanabe, H., and Ohta, S. (2005). Comparative study of the endocrine-disrupting activity of bisphenol A and 19 related compounds. *Toxicol. Sci* **84**, 249–259.

Kleymenova, E., Swanson, C., Boekelheide, K., and Gaido, K. W. (2005). Exposure in utero to di(n-butyl) phthalate alters the vimentin cytoskeleton of fetal rat sertoli cells and disrupts sertoli cell-gonocyte contact. *Biol. Reprod.* **73**, 482–490. 10.1095/biolreprod.104.037184.

Kokkinaki, M., Lee, T. L., He, Z. P., Jiang, J. J., Golestaneh, N., Hofmann, M. C., Chan, W. Y., and Dym, M. (2009). The molecular signature of spermatogonial stem/progenitor cells in the 6-day-old mouse testis. *Biol. Reprod.* **80**, 707–717.

Kuriyama, S. N., Talsness, C. E., Grote, K., and Chahoud, I. (2005). Developmental exposure to low-dose PBDE-99: Effects on male fertility and neurobehavior in rat offspring. *Environ. Health Persp.* **113**, 149–154.

Lakind, J. S., and Naiman, D. Q. (2011). Daily intake of bisphenol A and potential sources of exposure: 2005-2006 National Health and Nutrition Examination Survey. *J. Expo. Sci. Environ. Epid.* **21**, 272–279.

Lang, I. A., Galloway, T. S., Scarlett, A., Henley, W. E., Depledge, M., Wallace, R. B., and Melzer, D. (2008). Association of urinary bisphenol A concentration with medical disorders and laboratory abnormalities in adults. *Jama* **300**, 1303–1310.

Lassen, T. H., Frederiksen, H., Jensen, T. K., Petersen, J. H., Joensen, U. N., Main, K. M., Skakkebaek, N. E., Juul, A., Jorgensen, N., and Andersson, A. M. (2014). Urinary Bisphenol A levels in young men: association with reproductive hormones and semen quality. *Environ. Health Persp.* **122**, 478–484.

Lee, H. J., Chattopadhyay, S., Gong, E. Y., Ahn, R. S., and Lee, K. (2003). Antiandrogenic effects of bisphenol A and nonylphenol on the function of androgen receptor. *Toxicol. Sci.* **75**, 40–46.

Lee, S., Liu, X., Takeda, S., and Choi, K. (2013). Genotoxic potentials and related mechanisms of bisphenol A and other bisphenol compounds: A comparison study employing chicken DT40 cells. *Chemosphere*, **93**, 434–440. 10.1016/j.chemosphere.2013.05.029.

Lei, B., Xu, J., Peng, W., Wen, Y., Zeng, X., Yu, Z., Wang, Y., and Chen, T. (2016). In vitro profiling of toxicity and endocrine disrupting effects of bisphenol analogues by employing MCF-7 cells and two-hybrid yeast bioassay. *Environ. Toxicol.* doi: 10.1002/tox.22234.

Lie, P. P. Y., Mruk, D. D., Lee, W. M., and Cheng, C. Y. (2009). Epidermal growth factor receptor pathway substrate 8 (Eps8) is a novel regulator of cell adhesion and the blood-testis barrier integrity in the seminiferous epithelium. *Faseb J.* **23**, 2555–2567.

Liu, C., Duan, W., Li, R., Xu, S., Zhang, L., Chen, C., He, M., Lu, Y., Wu, H., Pi, H., *et al.* (2013). Exposure to bisphenol A disrupts meiotic progression during spermatogenesis in adult rats through estrogen-like activity. *Cell Death Dis.* **4**, e676. ARTN e67610.1038/cddis.2013.203.

Lucas, B. E., Fields, C., Joshi, N., and Hofmann, M. C. (2012). Mono-(2-ethylhexyl)-phthalate (MEHP) affects ERK-dependent GDNF signalling in mouse stem-progenitor spermatogonia. *Toxicology* **299**, 10–19.

Mahood, I. K., Scott, H. M., Brown, R., Hallmark, N., Walker, M., and Sharpe, R. M. (2007). In utero exposure to di(n-butyl) phthalate and testicular dysgenesis: comparison of fetal and adult end points and their dose sensitivity. *Environ. Health Perspect.* **115(Suppl 1)**, 55–61.

Marchetti, C., Walker, S. A., Odreman, F., Vindigni, A., Doherty, A. J., and Jeggo, P. (2006). Identification of a novel motif in DNA ligases exemplified by DNA ligase IV. *DNA Repair (Amst)* **5**, 788–798. 10.1016/j.dnarep.2006.03.011.

Martin, H. L., Adams, M., Higgins, J., Bond, J., Morrison, E. E., Bell, S. M., Warriner, S., Nelson, A., and Tomlinson, D. C. (2014). High-content, high-throughput screening for the identification of cytotoxic compounds based on cell morphology and cell proliferation markers. *PLoS One* **9**, e88338.

Melzer, D., Rice, N. E., Lewis, C., Henley, W. E., and Galloway, T. S. (2010). Association of urinary bisphenol A concentration with heart disease: evidence from NHANES 2003/06. *PloS One* **5**, e8673.

Nikolova, T., Dvorak, M., Jung, F., Adam, I., Kramer, E., Gerhold-Ay, A., and Kaina, B. (2014). The gamma H2AX assay for genotoxic and nongenotoxic agents: comparison of H2AX phosphorylation with cell death response. *Toxicol. Sci.* **140**, 103–117.

O'Brien, P. J., Irwin, W., Diaz, D., Howard-Cofield, E., Krejsa, C. M., Slaughter, M. R., Gao, B., Kaludercic, N., Angeline, A., Bernardi, P., *et al.* (2006). High concordance of drug-induced human hepatotoxicity with in vitro cytotoxicity measured in a novel cell-based model using high content screening. *Arch. Toxicol.* **80**, 580–604. 10.1007/s00204-006-0091-3.

Oatley, J. M., and Brinster, R. L. (2008). Regulation of spermatogonial stem cell self-renewal in mammals. *Annu. Rev. Cell Dev. Biol.* **24**, 263–286.

Pacchierotti, F., Ranaldi, R., Eichenlaub-Ritter, U., Attia, S., and Adler, I. D. (2008). Evaluation of aneugenic effects of bisphenol A in somatic and germ cells of the mouse. *Mutat. Res. Gen. Tox. En.* **651**, 64–70. 10.1016/j.mrgentox.2007.10.009.

Parks Saldutti, L., Beyer, B. K., Breslin, W., Brown, T. R., Chapin, R. E., Campion, S., Enright, B., Faustman, E., Foster, P. M., Hartung, T., *et al.* (2013). In vitro testicular toxicity models: Opportunities for advancement via biomedical engineering techniques. *Altex* **30**, 353–377.

Paul Friedman, K., Watt, E. D., Hornung, M. W., Hedge, J. M., Judson, R. S., Crofton, K. M., Houck, K. A., and Simmons, S. O. (2016). Tiered High-Throughput Screening Approach to Identify Thyroperoxidase Inhibitors Within the ToxCast Phase I and II Chemical Libraries. *Toxicol. Sci.* **151**, 160–180. 10.1093/toxsci/kfw034.

Perez, P., Pulgar, R., Olea-Serrano, F., Villalobos, M., Rivas, A., Metzler, M., Pedraza, V., and Olea, N. (1998). The estrogenicity of bisphenol A-related diphenylalkanes with various substituents at the central carbon and the hydroxy groups. *Environ. Health Perspect.* **106**, 167–174.

Perkins, E. J., Antczak, P., Burgoon, L., Falciani, F., Garcia-Reyero, N., Gutsell, S., Hodges, G., Kienzler, A., Knapen, D., McBride, M., *et al.* (2015). Adverse outcome pathways for regulatory applications: examination of four case studies with different degrees of completeness and scientific confidence. *Toxicol. Sci.* **148**, 14–25. 10.1093/toxsci/kfv181.

Persson, M., Loye, A. F., Mow, T., and Hornberg, J. J. (2013). A high content screening assay to predict human drug-induced liver injury during drug discovery. *J. Pharmacol. Tox. Met.* **68**, 302–313.

Pfeifer, D., Chung, Y. M., and Hu, M. C. T. (2015). Effects of low-dose bisphenol A on DNA damage and proliferation of breast cells: the role of c-Myc. *Environ. Health Perspect.* **123**, 1271–1279.

Radio, N. M., Breier, J. M., Shafer, T. J., and Mundy, W. R. (2008). Assessment of chemical effects on neurite outgrowth in PC12 cells using high content screening. *Toxicol. Sci.* **105**, 106–118.

Ramery, E., and O'Brien, P. J. (2014). Evaluation of the cytotoxicity of organic dust components on THP1 monocytes-derived macrophages using high content analysis. *Environ. Toxicol.* **29**, 310–319.

Repetto, G., del Peso, A., and Zurita, J. L. (2008). Neutral red uptake assay for the estimation of cell viability/cytotoxicity. *Nat. Protoc.* **3**, 1125–1131. 10.1038/nprot.2008.75.

Riu, A., Grimaldi, M., le Maire, A., Bey, G., Phillips, K., Boulahtouf, A., Perdu, E., Zalko, D., Bourguet, W., and Balaguer, P. (2011). Peroxisome proliferator-activated receptor gamma is a target for halogenated analogs of bisphenol A. *Environ. Health Perspect.* **119**, 1227–1232.

Rochester, J. R. (2013). Bisphenol A and human health: A review of the literature. *Reprod. Toxicol.* **42**, 132–155. 10.1016/j.reprotox.2013.08.008.

Roelofs, M. J. E., van den Berg, M., Bovee, T. F. H., Piersma, A. H., and van Duursen, M. B. M. (2015). Structural bisphenol analogues differentially target steroidogenesis in murine MA-10 Leydig cells as well as the glucocorticoid receptor. *Toxicology* **329**, 10–20.

Rogakou, E. P., Pilch, D. R., Orr, A. H., Ivanova, V. S., and Bonner, W. M. (1998). DNA double-stranded breaks induce histone H2AX phosphorylation on serine 139. *J. Biol. Chem.* **273**, 5858–5868.

Roukos, V., Pegoraro, G., Voss, T. C., and Misteli, T. (2015). Cell cycle staging of individual cells by fluorescence microscopy. *Nat. Protoc.* **10**, 334–348. 10.1038/nprot.2015.016.

Saffarini, C. M., Heger, N. E., Yamasaki, H., Liu, T., Hall, S. J., and Boekelheide, K. (2012). Induction and persistence of abnormal testicular germ cells following gestational exposure to di-(n-butyl) phthalate in p53-null mice. *J. Androl.* **33**, 505–513.

Sakaue, M., Ohsako, S., Ishimura, R., Kurosawa, S., Kurohmaru, M., Hayashi, Y., Aoki, Y., Yonemoto, J., and Tohyama, C. (2001). Bisphenol-A affects spermatogenesis in the adult rat even at a low dose. *J. Occup. Health* **43**, 185–190.

Schoonen, W. G. E. J., de Roos, J. A. D. M., Westerink, W. M. A., and Debiton, E. (2005). Cytotoxic effects of 110 reference compounds on HepG2 cells and for 60 compounds on HeLa, ECC-1 and CHO cells. II - Mechanistic assays on NAD(P)H, ATP and DNA contents. *Toxicol. In Vitro* **19**, 491–503.

Sidhu, J. S., Ponce, R. A., Vredevoogd, M. A., Yu, X. Z., Gribble, E., Hong, S. W., Schneider, E., and Faustman, E. M. (2006). Cell cycle inhibition by sodium arsenite in primary embryonic rat midbrain neuroepithelial cells. *Toxicol. Sci.* **89**, 475–484.

Sirenko, O., Mitlo, T., Hesley, J., Luke, S., Owens, W., and Cromwell, E. F. (2015). High-content assays for characterizing the viability and morphology of 3D cancer spheroid cultures. *Assay Drug Dev. Technol.* **13**, 402–414.

Sun, X., Kovacs, T., Hu, Y. J., and Yang, W. X. (2011). The role of actin and myosin during spermatogenesis. *Mol. Biol. Rep.* **38**, 3993–4001.

Tiwari, D., and Vanage, G. (2013). Mutagenic effect of Bisphenol A on adult rat male germ cells and their fertility. *Reprod. Toxicol.* **40**, 60–68.

Ullah, H., Jahan, S., Ain, Q. U., Shaheen, G., and Ahsan, N. (2016). Effect of bisphenol S exposure on male reproductive system of rats: A histological and biochemical study. *Chemosphere* **152**, 383–391.

Usman, A., and Ahmad, M. (2016). From BPA to its analogues: Is it a safe journey?. *Chemosphere* **158**, 131–142.

Vandenberg, L. N., Hauser, R., Marcus, M., Olea, N., and Welshons, W. V. (2007). Human exposure to bisphenol A (BPA). *Reprod. Toxicol.* **24**, 139–177.

Versaevel, M., Grevesse, T., and Gabriele, S. (2012). Spatial coordination between cell and nuclear shape within micropatterned endothelial cells. *Nat. Commun.* **3**, 671.

Vinggaard, A. M., Niemela, J., Wedebye, E. B., and Jensen, G. E. (2008). Screening of 397 chemicals and development of a quantitative structure-activity relationship model for androgen receptor antagonism. *Chem. Res. Toxicol.* **21**, 813–823. 10.1021/tx7002382.

Wang, H. F., Liu, M., Li, N., Luo, T., Zheng, L. P., and Zeng, X. H. (2016). Bisphenol A Impairs Mature Sperm Functions by a CatSper-Relevant Mechanism. *Toxicol. Sci.* **152**, 145–154.

Webster, M., Witkin, K. L., and Cohen-Fix, O. (2009). Sizing up the nucleus: nuclear shape, size and nuclear-envelope assembly. *J. Cell. Sci.* **122**, 1477–1486. 10.1242/jcs.037333.

Wegner, S., Hong, S., Yu, X., and Faustman, E. M. (2013). Preparation of rodent testis co-cultures. *Curr. Protoc. Toxicol.* Chapter 16, Unit 16 10, 10.1002/0471140856.tx1610s55.

Wegner, S., Yu, X., Kim, S., Harris, S., Griffith, W. C., Hong, S., and Faustman, E. M. (2014). Effect of dipentyl phthalate in 3-dimensional in vitro testis co-culture is attenuated by cyclooxygenase-2 inhibition. *J. Toxicol. Environ. Health Sci.* **6**, 161–169.

Wu, S., Wei, X. T., Jiang, J. J., Shang, L. Q., and Hao, W. D. (2012). Effects of bisphenol A on the proliferation and cell cycle of HBL-100 cells. *Food Chem. Toxicol.* **50**, 3100–3105.

Xiao, X., Mruk, D. D., Tang, E. I., Wong, C. K. C., Lee, W. M., John, C. M., Turek, P. J., Silvestrini, B., and Cheng, C. Y. (2014). Environmental toxicants perturb human Sertoli cell adhesive function via changes in F-actin organization mediated by actin regulatory proteins. *Hum. Reprod.* **29**, 1279–1291.

Xu, J. J., Diaz, D., and O'Brien, P. J. (2004). Applications of cytotoxicity assays and pre-lethal mechanistic assays for assessment of human hepatotoxicity potential. *Chem-Biol. Interact.* **150**, 115–128.

Xu, J. J., Henstock, P. V., Dunn, M. C., Smith, A. R., Chabot, J. R., and de Graaf, D. (2008). Cellular imaging predictions of clinical drug-induced liver injury. *Toxicol. Sci.* **105**, 97–105.

Yoshihara, S., Mizutare, T., Makishima, M., Suzuki, N., Fujimoto, N., Igarashi, K., and Ohta, S. (2004). Potent estrogenic metabolites of bisphenol A and bisphenol B formed by rat liver S9 fraction: Their structures and estrogenic potency. *Toxicol. Sci.* **78**, 50–59.

Yu, X., Faustman, E. M., Hong, S., and Sidhu, J. S. (2003). Effects of methyl mercury and cadmium on stress signaling and ubiquitination pathways in a primary Sertoli cell-gonocyte co-culture system. *Toxicol. Sci.* **72**, 274–274.

Yu, X. Z., Hong, S., Moreira, E. G., and Faustman, E. M. (2009). Improving in vitro Sertoli cell/gonocyte co-culture model for assessing male reproductive toxicity: Lessons learned from comparisons of cytotoxicity versus genomic responses to phthalates. *Toxicol. Appl. Pharmacol.* **239**, 325–336.

Yu, X. Z., Sidhu, J. S., Hong, S., and Faustman, E. M. (2005). Essential role of extracellular matrix (ECM) overlay in establishing the functional integrity of primary neonatal rat sertoli cell/gonocyte co-cultures: An improved In vitro model for assessment of male reproductive toxicity. *Toxicol. Sci.* **84**, 378–393.

Zhang, X. W., Chang, H., Wiseman, S., He, Y. H., Higley, E., Jones, P., Wong, C. K. C., Al-Khedhairy, A., Giesy, J. P., and Hecker, M. (2011). Bisphenol A disrupts steroidogenesis in human H295R cells. *Toxicol. Sci.* **121**, 320–327.

Zhang, Z. Z., Gong, Y. H., Guo, Y., Hai, Y. N., Yang, H., Yang, S., Liu, Y., Ma, M., Liu, L. H., Li, Z., *et al.* (2013). Direct transdifferentiation of spermatogonial stem cells to morphological, phenotypic and functional hepatocyte-like cells via the ERK1/2 and Smad2/3 signaling pathways and the inactivation of cyclin A, cyclin B and cyclin E. *Cell Commun. Signal.* **11**, 67.

Zhao, X. X., Toyooka, T., Kubota, T., Yang, G., and Ibuki, Y. (2015). gamma-H2AX induced by linear alkylbenzene sulfonates is due to deoxyribonuclease-1 translocation to the nucleus via actin disruption. *Mutat Res-Fund. Mol. M* **777**, 33–42.

Zhivotosky, B., and Orrenius, S. (2001). Assessment of apoptosis and necrosis by DNA fragmentation and morphological criteria. *Curr. Protoc. Cell Bio.l* Chapter 18, Unit 18 3, 10.1002/0471143030.cb1803s12.